Int J Earth Sci (Geol Rundsch) (2017) 106:2503–2525
DOI 10.1007/s00531-016-1444-7

ORIGINAL PAPER

Crustally derived granites in Dali, SW China: new constraints on silicic magmatism of the Central Emeishan Large Igneous Province

Bei Zhu[1] · David W. Peate[2] · Zhaojie Guo[3] · Runchao Liu[3] · Wei Du[3]

Received: 6 January 2016 / Accepted: 28 December 2016 / Published online: 6 March 2017

Abstract We have identified a new crustally derived granite pluton that is related to the Emeishan Large Igneous Province (ELIP). This pluton (the Wase pluton, near Dali) shows two distinct SHRIMP zircon U–Pb age groups (~768 and ~253 Ma). As it has an intrusive relationship with Devonian limestone, the younger age is interpreted as its formation, which is related to the ELIP event, whereas the ~768 Ma Neoproterozoic-aged zircons were inherited from Precambrian crustal component of the Yangtze Block, implying the pluton has a crustally derived origin. This is consistent with its peraluminous nature, negative Nb–Ta anomaly, enrichment in light rare earth elements, high $^{87}Sr/^{86}Sr_{(i)}$ ratio (0.7159–0.7183) and extremely negative $\varepsilon(Nd)_{(i)}$ values (−12.15 to −13.70), indicative of melts derived from upper crust materials. The Wase pluton-intruded Devonian strata lie stratigraphically below the Shangcang ELIP sequence, which is the thickest volcanic sequence (~5400 m) in the whole ELIP. The uppermost level of the Shangcang sequence contains laterally restricted rhyolite. Although the rhyolite has the same age as the Wase pluton, its geochemical features demonstrate a different magma origin. The rhyolite displays moderate $^{87}Sr/^{86}Sr_{(i)}$ (0.7053), slightly negative $\varepsilon(Nd)_{(i)}$ (−0.18) and depletions in Ba, Cs, Eu and Sr, implying derivation from differentiation of a mantle-derived mafic magma source. The coexistence of crustally and mantle-derived felsic systems, along with the robust development of dike swarms, vent proximal volcanics and thickest flood basalts piles in Dali, shows that the Dali area was probably where the most active Emeishan magmatism had once existed.

Keywords Emeishan · Large Igneous Province · Dali · Granite · Crustal melting

Introduction

Although large igneous provinces (LIPs) are commonly known for their voluminous and rapidly emplaced flood basalt formations, silicic plutonic rocks, which are much smaller in proportion, can comprise a significant component in LIP systems (Bryan and Ernst 2008; Bryan et al. 2010). They carry important information on magma evolution and the petrogenetic processes that create a LIP event. The widely accepted mantle plume theory attributes the generation of LIPs to large-scale decompressional melting of a deep hot mantle plume when it rises to the base of lithosphere (e.g. White and McKenzie 1989; Campbell and Griffiths 1990; Griffiths and Campbell 1990, 1991; Campbell 2005, 2007). The evolution of primary, mantle-derived mafic magma can produce subordinate silicic magma either by fractional crystallization (Loiselle and Wones 1979; Turner et al. 1992; Peccerillo et al. 2003; Shellnutt and Zhou 2007; Zhong et al. 2007) or by partial melting of the fractionated cumulates (Shellnutt and Zhou 2007, 2008; Zhou et al. 2008). Alternatively, the high temperature of

Electronic supplementary material The online version of this article (doi:10.1007/s00531-016-1444-7) contains supplementary material, which is available to authorized users.

✉ Zhaojie Guo
zjguo@pku.edu.cn

[1] School of Geoscience and Technology, Southwest Petroleum University, Chengdu 610500, Sichuan, China

[2] Department of Earth and Environmental Sciences, University of Iowa, Iowa City, IA 52242, USA

[3] Key Laboratory of Orogenic Belts and Crustal Evolution, Ministry of Education, School of Earth and Space Sciences, Peking University, Beijing 100871, China

underplated mafic magma can also trigger melting of the overlying crust materials, resulting in formation of crustally derived silicic magma (White and McKenzie 1989; Campbell and Griffiths 1990; Zhong et al. 2007; Shellnutt et al. 2011a). Silicic lithologies derived from these magma series not only introduce robust diversity to the petrogenetic processes on the Earth, but also provide essential constraints on details of individual LIPs, such as ages, eruption stage and potential effect to the environment (He et al. 2007; Bryan et al. 2010; Xu et al. 2010; Zhong et al. 2011, 2014; Shellnutt et al. 2012).

The middle Permian Emeishan Large Igneous Province (ELIP) located in the western Yangtze Block (SW China) is a typical intraplate LIP that is regarded as related to mantle plume activities (Fig. 1a) (Chung and Jahn 1995Xu et al. 2001; Ali et al. 2005; Zhang et al. 2006, 2009; Shellnutt 2014). The Indo–Eurasia collision has eliminated most of the western portion of the ELIP, but volcanic and plutonic rocks located in North Vietnam are interpreted as dislocated units (Hanski et al. 2004; Anh et al. 2011; Tran et al. 2015; Usuki et al. 2015). As a consequence of this tectonic event, the plume center of the ELIP (the 'Central ELIP') is now in direct contact with the eastern frontier of the Tibetan orogenic regime (Chung and Jahn 1995; Chung et al. 1998; Shellnutt 2014). This tectonic activity has resulted in robust exhumation of abyssal plutons of the Central ELIP, thereby making the ELIP one of the best places to study plume-related silicic magmatism (Zhong et al. 2011). However, due to control by a regional N–S structural lineament, the exhumed plutons are mostly confined to the linear area between the cities of Panzhihua and Xichang (i.e. the Panxi paleo-rift) (Fig. 1a; Table 1). ELIP-related silicic intrusions have rarely been reported outside this Panxi paleo-rift.

In this article, we report the finding of a new ELIP-related pluton in the Wase town of the Dali area, which is located outside the Panxi paleorift, ~200 km south of Panzhihua City. In contrast to the Panxi paleo-rift plutons that are mostly found as highly fragmented tectonic complexes,

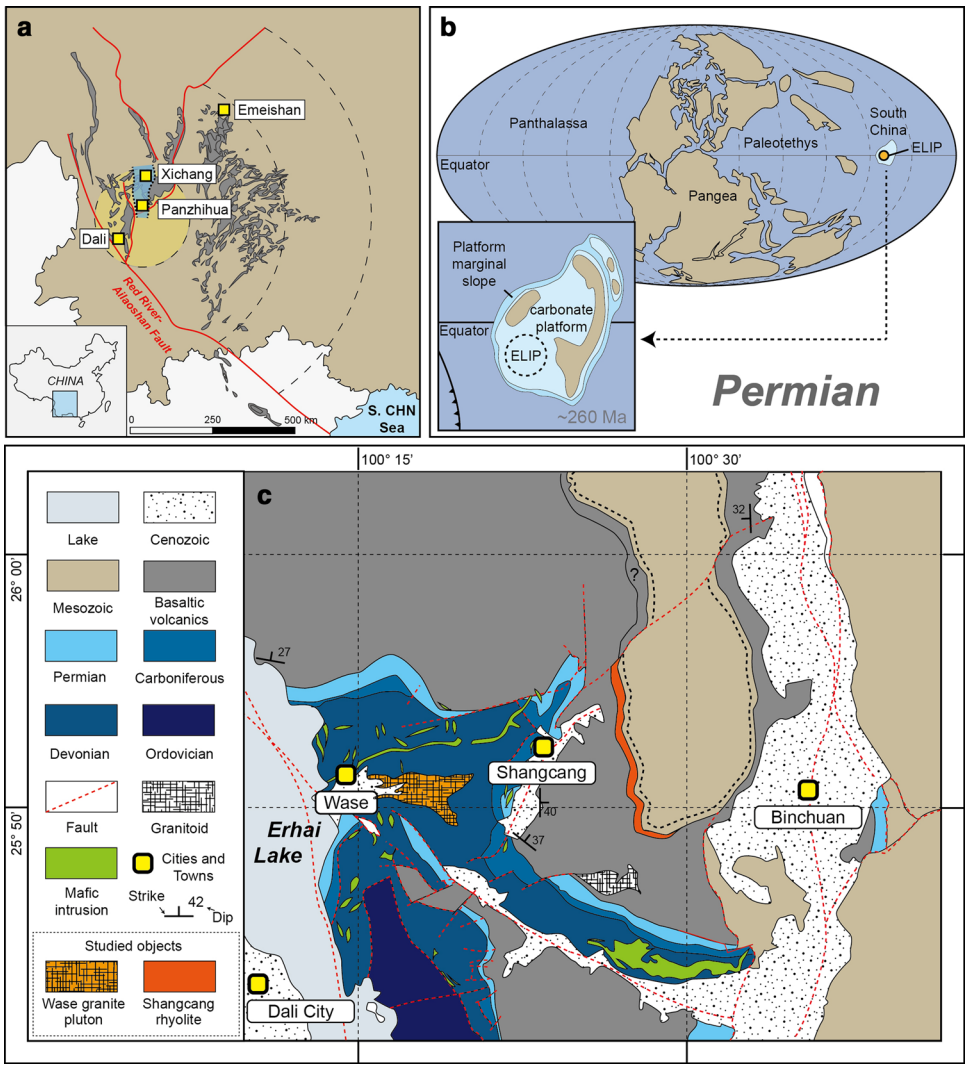

Fig. 1 Tectonic background of the ELIP; **a** distribution of extant exposures of the ELIP system (after Sun et al. 2010); **b** location of Yangtze Block in the Permian (after Jerram et al. 2016); **c** geological map of the Dali area showing locations of the Wase pluton and the Shangcang rhyolite (after Zhu et al. 2014)

Table 1 Summary of reported granitoid plutons in the Panxi area, Central ELIP

Location	Petrological featuress			Chronology		Sr–Nd isotope spectrometry			Petrogenetic mechanism
From N to S	Lithology	A/CNK	References	U–Pb ages (Ma)	References	$^{87}Sr/^{86}Sr_{(i)}$ range	$\varepsilon(Nd)_{(i)}$ range	References	
Taihe	Granite	Peralkaline	Shellnutt and Zhou (2007)	261.4 ± 2.3	Xu et al. (2008)	0.6848–0.6978	+1.5 to +1.8	Shellnutt and Zhou (2007)	Mantle-derived; from fractional crystallization of mafic magma (Shellnutt and Zhou 2007)
Cida	Granite	Peralkaline	Zhong et al. (2007)	258.4 ± 0.6	Shellnutt et al. (2012)	0.7023–0.753	−0.25 to +0.24	Zhong et al. (2007)	Mantle-derived; from fractional crystallization of mafic magma (Zhong et al. (2007)
Huangcao	Fayalite syenite	Metaluminous	Shellnutt et al. (2012)	258.9 ± 0.7	Shellnutt et al. (2012)	0.7045–0.7068	+1.3 to +1.9	Shellnutt and Zhou (2008)	Mantle-derived, from partial melting of gabbroic cumulates (Shellnutt and Zhou, 2008)
Woshui	Syenite	Metaluminous	Shellnutt and Zhou (2007)	259.6 ± 0.5	Shellnutt et al. (2012)	0.7043–0.7044	+2.6 to +3.1	Shellnutt and Zhou (2007)	Mantle-derived, from partial melting of gabbroic cumulates (Shellnutt and Zhou 2007)
Baima	Syenite	Peralkaline	Zhou et al. (2008)	262 ± 2	Zhou et al. (2008)	0.7044–0.7078	+0.6 to +1.8	Zhou et al. (2008)	Mantle-derived; from fractional crystallization of mafic magma (Zhou et al. (2008)
Maomaogou	Nephline syenite	Metaluminous	Luo et al. (2007)	261.6 ± 4.4	Luo et al. (2007)	N/A	−0.73 to 1.36	Luo et al. (2007)	Mantle-derived, from partial melting of gabbroic cumulates (Luo et al. (2007)
Salian	Diorite	Metaluminous	Xu et al. (2008)	260.4 ± 3.6	Xu et al. (2008)	N/A	N/A	N/A	Mantle-derived; from fractional crystallization of mafic magma (Xu et al. (2008)

Table 1 (continued)

Location	Petrological featuress			Chronology		Sr–Nd isotope spectrometry			Petrogenetic mechanism
From N to S	Lithology	A/CNK	References	U–Pb ages (Ma)	References	$^{87}Sr/^{86}Sr_{(i)}$ range	$\varepsilon(Nd)_{(i)}$ range	References	
Panzihua	Granite	Peralkaline	Shellnutt and Jahn (2010)	N/A	N/A	0.6963–0.7037	+2.2 to +2.9	Shellnutt and Zhou 2007)	Mantle-derived; from fractional crystallization of mafic magma (Shellnutt and Zhou 2007)
Daheishan	Syenite	Metaluminous	Zhong et al. (2009)	259.1 ± 0.5	Shellnutt et al. (2012)	0.7040–0.7050	+2.37 to +3.25	Zhong et al. (2009)	Mantle-derived, from partial melting of gabbroic cumulates (Zhong et al. (2009)
Yingpanliangzi	Granite	Peraluminous	Shellnutt et al. (2011a, b)	260 ± 8; 882 ± 22	Shellnutt et al. (2011a, b)	0.71074–0.71507	−3.9 to −4.4	Shellnutt et al. (2011a, b)	Crustally-derived; from partial melting of the Yangtze crust
Ailanghe	Granite	Peraluminous	Zhong et al. (2007)	256.2 ± 3.0; 256.8 ± 2.8	Zhong et al. (2011)	0.7102–0.7111	−6.34 to −6.26	Zhong et al. (2007)	Crustally-derived; from partial melting of the Yangtze crust (Zhong et al. (2007)

the Wase pluton is closely associated with a well-developed, continuous late Paleozoic stratigraphic section. The Permian part of this section preserves the thickest Emeishan volcanic sequence in the whole ELIP (the famous ~5400 m thick Shangcang Section) and notably contains laterally restricted silicic extrusions (Shangcang rhyolite) in its uppermost part (Xu et al. 2001, 2010; He et al. 2007; Zhu et al. 2014). The good geological conditions provide an opportunity to evaluate the relationship between the intrusive and extrusive system of the silicic magmatism. We provide new data from SHRIMP U–Pb geochronology, bulk rock geochemistry and Sr–Nd isotope mass spectrometry of the Wase pluton and Shangcang rhyolite to reveal their petrologic characteristics and petrogenetic origin. By comparing their petrological and geochemical characteristics, we examine whether the newly recognized Wase pluton has any genetic links with the overlying Shangcang silicic volcanics.

Geological background

The ELIP was developed on the Yangtze Block, a major tectonic unit that constitutes the modern Southwest China (Shellnutt 2014). Specifically, the 'Upper Yangtze Block' refers to the west part of the Yangtze block that contains the Yunnan, Guizhou and Sichuan Provinces. It is separated from the Tibetan orogenic regime by the Red River-Ailaoshan-Longmenshan thrust fault system (Fig. 1a). The basement materials of the Yangtze Block were formed during the Archean to Early Neoproterozoic times (e.g. Zhou et al. 2002). They were fully cratonized after the ~1000 to 820 Ma Jinning-Sibao orogenic event. The last Precambrian tectono-magmatic event of the Upper Yangtze Block occurred in Late Neoproterozoic times. In the western Upper Yangtze Block, granites formed during this time (e.g. the Kangding Granites) can often be observed intruding into the Pre-Neoproterozoic metamorphosed complex (e.g. Zhou et al. 2002; Ling et al. 2003). Two different models have been proposed to account for this tectonic activity. One view argues that it was an episode of rifting related to the break-up of the Rodinia super continent, of which the Yangtze block was once a part (Li et al. 2002, 2003, 2006; Zheng et al. 2007). The other opinion attributes the generation of the Neoproterozoic magmatism to subduction; suggesting that the tectonic setting was a volcanic arc environment (Zhou et al. 2002, 2006a, b; Shen et al. 2003; Wang et al. 2007; Sun et al. 2009).

From late Neoproterozoic to Triassic, the Upper Yangtze Block was isolated from the main Gondwana continent and surrounded by an oceanic environment. Sedimentary covers began to develop on its crustal basement (Fig. 1b). The first sedimentary system developed after the basement-forming age is a suite of un-metamorphosed or weakly metamorphosed slate, siltstone or shale formations, in which detrital zircons with minimum ages of ~700 to 800 Ma are found. Representative sedimentary systems formed during this period include the Liantuo Formation (Lan et al. 2015), the Chengjiang Formation (Wang et al. 2012), the Banxi Group (Lan et al. 2015), the Lieguliu Formation and the Guanyinya Formtaion (Sun et al. 2009). This initial sedimentary cover is successively overlain by a thick sequence formed from Sinian to Phanerozoic times. Based on paleomagnetic, paleontological and paleogeographic data (Fig. 1b), it was suggested that the Yangtze Block was located in the equatorial area and was affected by regional marine transgression during the late Paleozoic (Wu et al. 2015). As a consequence, it was submerged under a shallow submarine environment. A vast carbonate platform, therefore, was developed on the surface of the Yangtze Block (Fig. 1b). During the middle Permian, the ELIP broke out on the Upper Yangtze Block. Abundant volcanic materials erupted at the surface, interrupting the continuous sedimentation of the carbonate platform. During the ELIP event, the environment changed from shallow-water submarine to overwhelmingly terrestrial (Zhu et al. 2014). The terrestrial environment was characterized by the voluminous piles of the Emeishan flood basalts.

The precise age of the ELIP event, based on more than 50 U–Pb and Ar–Ar dates, is ~260 Ma (Shellnutt et al. 2012; Table 1 in; Shellnutt 2014 and references therein), coincident with the end-Guadalupian mass extinction (Zhou et al. 2002; Wignall et al. 2009). The modern outcrop of the ELIP is roughly estimated ~2.5×10^5 km^2 (e.g. Ali et al. 2005) (Fig. 1a), forming a rhombic area in SW China. The Dali area is located in the southwest part of the central ELIP. It is characterized by the ~5400 m Shangcang volcanic sequence (Fig. 1c), which is significantly thicker than any other volcanic sequence in the whole ELIP (average thickness ~700 m: Ali et al. 2005). Zhu et al. (2014) divided the Shangcang volcanic sequence into three subordinate successions and consequently interpreted them as a shoaling cycle from subaqueous volcanism to subaerial lava-effusion. The ~200 to 300 m lowermost part (Basal Succession) is dominated by pillow lava piles, indicating that the earliest phase formed in a relatively deep subaqueous environment. The lower ~2400 m (Lower Succession) is characterized by explosive hydromagmatic deposits, indicating that the early stage of the local Emeishan volcanism was mainly activated in a shallower subaqueous environment. The upper ~2700 m (Upper Succession) consists of terrestrial flood basalt lavas interlayered with subaerial fallout tuff, indicating that the main phase of local volcanism erupted in a subaerial environment (Fig. 2). It should be noted that two extrusive silicic units are found in the uppermost ~900 m of the Upper Succession. This sequence

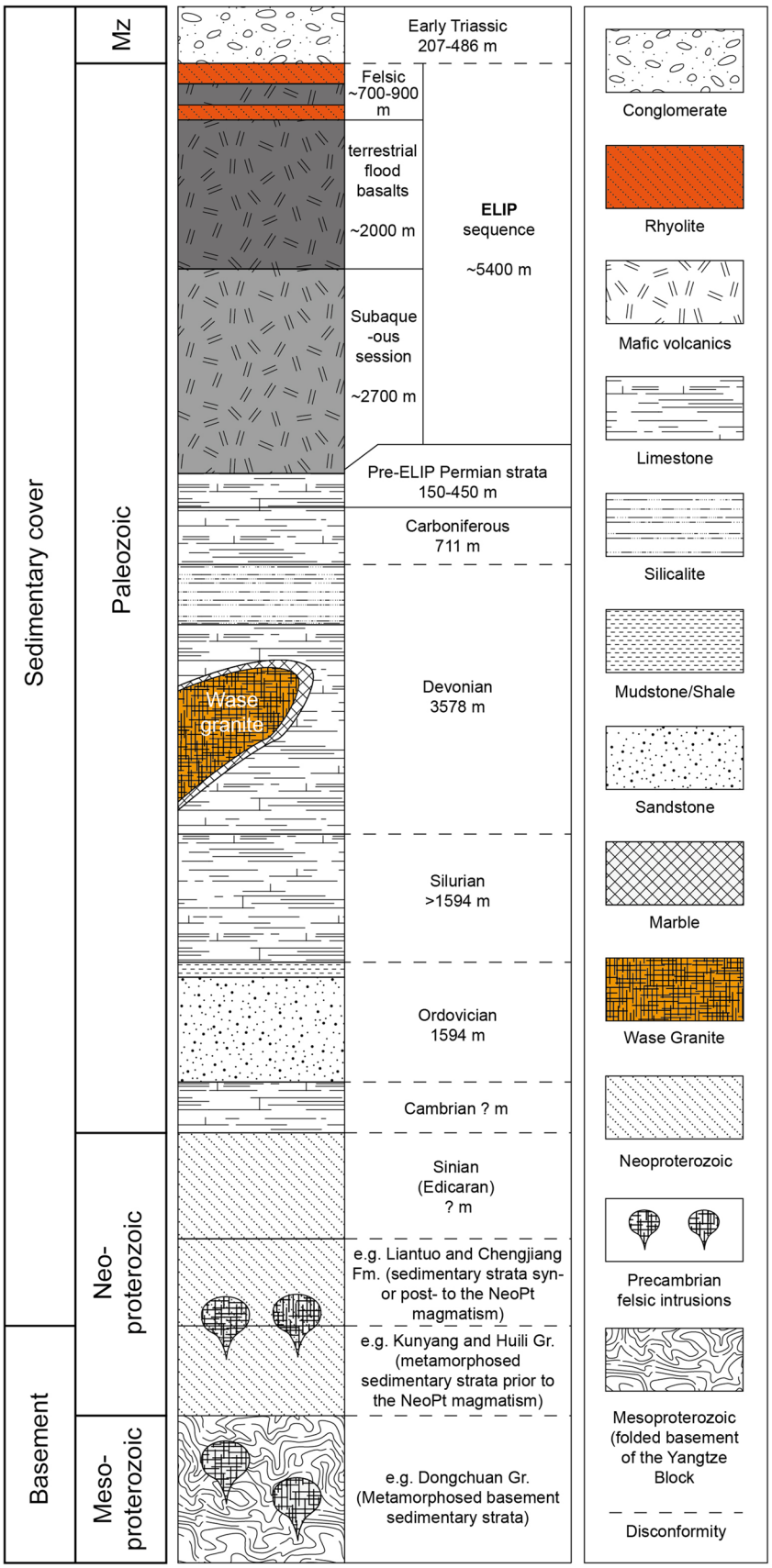

Fig. 2 A summary stratigraphic column (Precambrian to Paleozoic) for the Upper Yangtze Block. Thickness and stratigraphic data are from YBG (1966, 1973); Chen and Jahn (1998); Zhou et al. (2002); Sun et al. (2009); Wang et al. (2012) and Lan et al. (2015)

contains a lower ~200 m thick well-banded rhyolite unit, overlain by ~500 m basalt lavas, and then succeeded by ~200 m of porphyritic rhyolite (Xu et al. 2001, 2010; Zhu et al. 2014) (Fig. 2). The lateral extension of these silicic lavas is restricted to the Dali area. Away from the Dali area, silicic lavas are generally absent in the uppermost part of the ELIP sequence, where the lithological assemblage changes to sections intercalated between flood basalts and Wuchiapingian sedimentary layers [YBG (Yunnan Bureau of Geology) 1966, 1977; RSWY (Regional Stratigraphic Workgroup of Yunnan), 1978].

The Wase granitic pluton is located about ~5 km west of the Shangcang section (Fig. 1c). Geologically, the Wase pluton is in direct contact with the Devonian carbonate sequence below the Permian and Carboniferous section of the local stratigraphy (Fig. 2). The exposure of the Wase pluton limits the exhumation of the early Paleozoic in the local area, but in adjacent places (e.g. Changhai-Heqing area to the north or Xiaguan area to the south), Ordovician and Silurian strata have been recognized (YBG 1966, 1973) (Fig. 2).

Field structure and petrography

Wase granite

The Wase pluton is in direct contact with the Devonian limestone strata (Figs. 1c, 2) with no clay or brecciated materials at the contact. A ~2 m wide zone of limestone adjacent to the pluton is generally metamorphosed to marble and contains lighter-toned, fully recrystallized calcite crystals that show no trace of any sedimentary structures (Fig. 3a–c). Moving outwards, the proportion of marble sharply decreases, and the lithology gradually transitions into primary limestone deposits in which original sedimentary bedding is well preserved (Fig. 3a). The bedding plane of the limestone laminations obliquely intersects the orientation of the granite–marble boundary (Fig. 3a).

The marginal area of the granite pluton is light grey in colour and consists of medium- to coarse-grained feldspar and quartz mingled in massive structure. In contrast, the core of the pluton is reddish in colour with a coarse-grained texture (Fig. 3d, e). We collected two samples from the core (HD-15) and marginal (DL-07) areas of the Wase pluton. Both samples are very fresh, as indicated by low loss on ignition (LOI) values (<1 wt%) and the lack of hydrothermal or metamorphic overprinting in thin section (Fig. 3d, e). The core sample (HD-15) is composed of ~34% quartz, ~30% alkali feldspar, ~27% plagioclase, ~9% biotite and minor accessory phases like zircon and apatite (Fig. 3d, e). The marginal DL-07 sample is made up of ~37% quartz, ~45% alkali feldspar, ~18% plagioclase, ~1% calcite and minor accessory phases—zircon and apatite (Fig. 3d, e). Both samples display granitic textures in which the plagioclase crystals are subhedral with 120-degree triple junctions (Fig. 3d, e). The quartz grains are generally subhedral to anhedral in shape with irregular boundaries (Fig. 3d, e). Medium- to coarse-sized grains are predominant in proportion, but some fine-sized quartz can be observed adjacent to the rims of some larger crystals (Fig. 3d, e).

Shangcang rhyolite

There is a ~200 m thick sequence of porphyritic rhyolites located in the uppermost part of the ~5400 m Shangcang ELIP sequence, which was previously investigated by Xu et al. (2010). We collected two samples [DL-32(2) and DL-32(3)] from the uppermost part of the rhyolite unit, ~5 to 6 m below the upper stratigraphic boundary of the Shangcang ELIP sequence. The rhyolite exhibits a massive to columnar-jointed structure. It contains ~20 to 30% euhedral quartz and feldspar phenocrysts (~2 to 7 mm in diameter) set in a dark red, cryptocrystalline matrix (Fig. 3f). Under microscopic observation, it can be seen that the phenocrysts are surrounded by well-developed fluidal patterns of the matrix that is made up of a fine mixture of elongated micro-vesicles and welded hyalocrystalline to cryptocrystalline materials together with about 10% Fe–Ti oxide grains (Fig. 3f). Broken crystal debris, cognate volcaniclasts and accidental lithic shards are rare in the rhyolite, indicating that it is unlikely to be an ignimbrite.

Analytical methods

SHRIMP U–Pb geochronology

In order to date the Wase pluton and Shangcang rhyolite, zircons were separated from the sample powders of HD-15 (Wase pluton) and DL32 (Shangcang rhyolite) using conventional heavy liquids. After mounting in epoxy, the zircons were examined under transmitted light, reflected light and cathodoluminescence (CL) in order to avoid crystals that have fractures or inclusions. U–Pb isotope analysis of the selected zircons was performed with a SHRIMP-II at the Institute of Geology, Chinese Academy of Geological Sciences, on gold-coated mounts using the procedure described by Williams (1998). The standard sample TEMORA 1 (~417 Ma, Black et al. 2003) was chosen to monitor inter-element fractionation. Common Pb corrections followed the procedure described by Compston et al. (1984). The data are given in Table 2. Uncertainties of individual analyses are reported at 1-sigma level. The weighted mean age of the test is given at 95% confidence level. The calculation of the weighted mean age and plotting of the

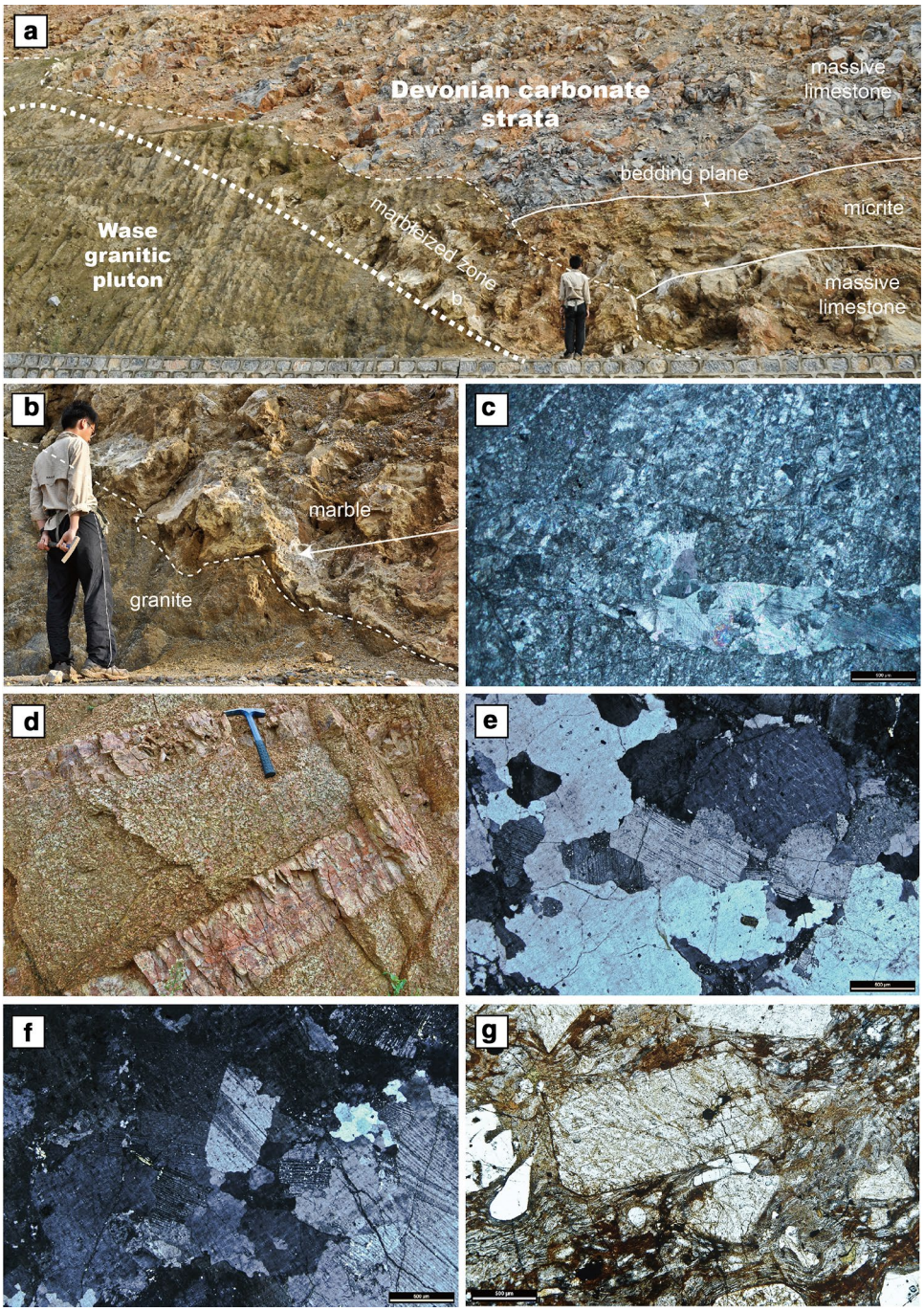

Fig. 3 Field and petrographic observations of the Wase pluton and the Devonian limestone contact rock; **a** wide view showing the contact relationship of the Wase pluton and the Devonian; **b** a marbleized zone is developed at the lithological boundary, which is clear and sharp without any secondary materials at the contact; **c** microscope image of the marble; **d** close-up view of the Wase pluton, showing the coarse-grained granite (sample HD-15) cut by fine-grained felsic intrusions; **e, f** microscope images of the Wase granite; **g** microscope image of the Shangcang rhyolite

Concordia were made using ISOPLOT/Ex4.15 (Ludwig 2012).

Bulk-rock geochemistry

Major elements of samples HD-15, DL-07, DL-32(2) and DL-32(3) were analyzed using an AXIOS-PW4400 X-ray fluorescence spectrometer in the Chinese Academy of Geological Sciences. Trace elements were analyzed using a PE300D inductively coupled plasma–mass spectrometer (ICP–MS) in the Institute of Geology, Chinese Academy of Geological Sciences, on powders digested with $HF+HNO_3$ acids. The data are given in Table 3.

Sr–Nd isotope mass spectrometry

Sr–Nd isotope measurements were made on HD-15, DL-07 and DL-32(3) following the methods of Li et al. (2011, 2012). After dissolving the powdered sample with $HF+HNO_3+HClO_4$ in Teflon capsules, Sr and Nd were

Table 2 Results of the SHRIMP zircon U–Pb analysis of the Wase pluton

Spot	$^{206}Pb_c$ (%)	U (ppm)	Th (ppm)	$^{232}Th/^{238}U$	$^{206}Pb^*$ (ppm)	$^{207}Pb^*/^{206}Pb^*$	Error% (1σ)	$^{207}Pb^*/^{235}U$	Error% (1σ)	$^{206}Pb^*/^{238}U$	Error% (1σ)	$^{206}Pb/^{238}U$ age	
HD15-1	0.63	266	121	0.47	9.43	0.0459	8	0.26	8.2	0.041	1.4	259	±3.6
HD15-2	–	508	484	0.99	55.4	0.06457	1	1.132	1.5	0.1272	1.1	771.8	±8.2
HD15-3	0.25	459	340	0.76	52.1	0.06226	1.4	1.13	1.8	0.1317	1.1	797.3	±8.5
HD15-4	0.24	262	146	0.58	28.1	0.0633	1.8	1.088	2.2	0.1246	1.2	756.9	±8.7
HD15-5	1.32	233	86	0.38	8.4	0.0454	8	0.26	8.2	0.04148	1.5	262	±3.8
HD15-6	0.00	940	131	0.14	102	0.06445	0.77	1.125	1.3	0.1266	1.1	768.4	±7.8
HD15-7	0.15	283	160	0.58	32.3	0.0642	1.8	1.173	2.2	0.1325	1.2	802.3	±9.3
HD15-8	0.13	303	383	1.30	31.3	0.06408	1.4	1.061	1.9	0.1201	1.3	731.1	±8.7
HD15-9	0.07	245	86	0.36	26.5	0.065	1.8	1.127	2.2	0.1258	1.3	763.9	±9.1
HD15-10	0.37	121	100	0.85	12.9	0.0657	2.5	1.117	3.3	0.1233	2.2	749	±16
HD15-11	0.00	132	74	0.58	4.41	0.0556	3.9	0.299	4.3	0.03899	1.8	246.6	±4.4
HD15-12	0.72	324	199	0.64	40.1	0.0617	2.8	1.218	3.2	0.1431	1.5	862	±12
HD15-13	2.30	251	153	0.63	51.8	0.0563	9.5	1.83	9.6	0.2351	1.6	1361	±20
HD15-14	0.23	360	142	0.41	39.2	0.063	2.1	1.1	2.4	0.1265	1.2	768.1	±8.6
HD15-15	0.22	295	139	0.49	32.5	0.0665	1.6	1.172	2	0.1279	1.2	775.7	±9.1
DL32(3)-1	2.06	90	47	0.54	3.14	0.0368	15	0.203	15	0.03991	2	252.3	±4.9
DL32(3)-2	0.62	199	92	0.48	7.05	0.0481	5.4	0.271	5.6	0.04091	1.5	258.5	±3.8
DL32(3)-3	0.79	102	50	0.51	3.51	0.0491	12	0.271	13	0.03995	1.9	252.5	±4.8
DL32(3)-4	–	94	42	0.47	3.2	0.0602	4.2	0.332	4.6	0.03995	1.8	252.5	±4.6
DL32(3)-5	1.34	109	50	0.48	3.76	0.0477	13	0.26	13	0.03961	1.9	250.4	±4.7
DL32(3)-6	1.29	104	50	0.50	3.52	0.0496	8	0.265	8.2	0.03875	1.8	245.1	±4.4
DL32(3)-7	0.36	102	44	0.44	3.49	0.0574	7.8	0.312	8	0.03951	1.8	249.8	±4.5
DL32(3)-8	1.29	117	70	0.62	4.07	0.0458	9	0.253	9.2	0.04011	1.8	253.5	±4.5
DL32(3)-9	2.34	78	48	0.63	2.68	0.04	23	0.214	23	0.03876	2.3	245.1	±5.5
DL32(3)-10	–	115	57	0.51	3.83	0.0585	4.1	0.314	4.5	0.03892	1.8	246.1	±4.3
DL32(3)-11	–	132	60	0.46	4.55	0.0562	3.9	0.311	4.4	0.04009	1.8	253.4	±4.6
DL32(3)-12	0.34	140	63	0.47	5.13	0.0487	5.9	0.284	6.2	0.04239	1.8	267.6	±4.7
DL32(3)-13	0.71	107	77	0.74	3.86	0.0478	7.1	0.276	7.4	0.04186	1.8	264.4	±4.6
DL32(3)-14	0.82	116	54	0.48	4.12	0.0498	11	0.28	11	0.04084	1.9	258	±4.7
DL32(3)-15	0.34	150	73	0.50	5.11	0.0517	5.1	0.281	5.4	0.03945	1.6	249.4	±4.0
DL32(3)-16	–	104	54	0.54	3.54	0.0568	4.5	0.311	4.8	0.03964	1.8	250.6	±4.5
DL32(3)-17	0.23	273	133	0.50	9.4	0.0513	3.2	0.282	3.5	0.03994	1.4	252.4	±3.4
DL32(3)-18	3.63	87	46	0.54	3.23	0.0423	30	0.244	30	0.0418	2.6	263.9	±6.8

The $^{206}Pb^*$ and $^{206}Pb_c$ represent radiogenic and common Pb, respectively. ^{204}Pb method was used to correct the common Pb

Table 3 Results of the major and trace element analysis of the Wase pluton and the Shangcang rhyolite

Sample	DL-07	HD-15	RL-32(2)	RL-32(3)
Location	Wase	Wase	Shangcang	Shangcang
SiO_2	80.13	76.34	70.97	70.13
TiO_2	0.08	0.08	0.44	0.45
Al_2O_3	10.59	12.32	13.43	13.22
Fe_2O_3	0.61	0.81	2.72	4.41
FeO*	0.23	0.13	0.45	0.2
MnO	0.01	0.01	0.01	0.08
MgO	0.26	0.2	0.2	0.24
CaO	0.26	0.35	0.35	0.14
Na_2O	2.97	3.3	3.3	2.36
K_2O	4.1	5.23	6.95	6.79
P_2O_5	0.02	0.02	0.06	0.04
LOI	0.89	0.74	1.39	1.58
Total	99.92	99.4	99.82	99.44
V	9.08	4.65	6.78	6.21
Cr	7.68	5.32	4.68	7.37
Co	1.6	0.59	1.77	2.07
Ni	3.37	2.42	3.06	4.64
Cu	33.4	1.58	5.63	5.91
Zn	9.14	8.46	133	117
Ga	10.5	13.7	38	38
Rb	86.9	109	127	127
Sr	61.5	118	33.6	39.4
Y	5.94	5.47	89.3	97.3
Zr	61.1	55.7	977	1020
Nb	4.99	2.99	135	136
Cs	1.04	0.52	0.21	0.3
Ba	602	765	340	362
La	9.54	7.17	180	154
Ce	16.6	17.8	309	339
Pr	1.96	1.52	39.8	36
Nd	6.85	5.38	144	128
Sm	1.51	1.23	27.2	24.9
Eu	0.32	0.38	2.29	2.26
Gd	1.05	0.88	22.2	20.7
Tb	0.18	0.14	3.64	3.5
Dy	1.04	0.87	18.7	19.2
Ho	0.21	0.19	3.54	3.7
Er	0.72	0.61	10.9	11.1
Tm	0.11	0.09	1.41	1.45
Yb	0.91	0.7	9.52	9.85
Lu	0.15	0.12	1.47	1.49
Hf	2.05	1.74	23.4	23.9
Ta	0.57	0.16	7.47	7.77
Pb	3.26	6.72	17.2	13.2
Th	5.67	4.45	21.5	24.4
U	0.79	1.41	4.58	5.68
La_N/Yb_N	7.07	6.91	12.75	10.54
La_N/Sm_N	3.97	3.67	4.16	3.89
Gd_N/Yb_N	0.93	1.01	1.88	1.7
Eu/Eu*	0.74	1.07	0.28	0.3

REE normalization was performed using the C1 chondrite data from Boynton (1984). The normalized element concentrations are marked with a subscript 'N'. Eu/Eu* = $[2Eu^*/(Sm_N + Gd_N)]$

separated by ion exchange chromatography, and analyzed on a Thermofisher Triton Plus Multi-collector Thermal Ionization Mass Spectrometer (TIMS) in the Institute of Geology and Geophysics, Chinese Academy of Sciences. The $^{88}Sr/^{86}Sr$ and $^{146}Nd/^{144}Nd$ ratios were normalized to 8.375209 and 0.7219, respectively for mass fractionation correction. Two international standard samples, NBS-987 and JNdi-1, were used to check instrument stability during the measurement and their values are given along with the results of the measured samples in Table 4. Data accuracy was monitored by analyzing BCR-2, a USGS reference material, which gave $^{87}Sr/^{86}Sr = 0.705011 \pm 0.000008$ and $^{143}Nd/^{144}Nd = 0.512632 \pm 0.000010$, values that are in good agreement with previous TIMS analyses reported by Li et al. (2011, 2012).

Results

U–Pb geochronology

Wase granite

A total of 15 individual zircon U–Pb analyses were made for sample HD-15, and their CL images are shown in Fig. 4a. The grains are clear and euhedral, and the majority have an obvious core, mantled by a fine oscillatory zoning pattern. These characteristics indicate an igneous origin, which is further supported by the Th/U ratio (0.36–0.99) of the zircon grains, except for the spot HD15-8, which shows a higher value of 1.30 and thus is excluded from the following age calculation (Table 2).

The age calculation of the remaining zircon grains was made based on their $^{206}Pb/^{238}U$ ratios. Among these grains, HD15-3 is apparently discordant and excluded from age calculation. HD15-7, 12, 13 exhibit obviously older ages at 802.3 ± 9.3, 862.3 ± 12.4 and 1361.4 ± 19.6 Ma, respectively. The rest of the zircon grains concentrate into two age groups. One group, which is made up of 7 spots, displays a weighted mean $^{206}Pb/^{238}U$ age of ~768.0 ± 8.7 Ma (MSWD = 0.61); whereas the other group, which is made up of 3 individual analysis results, yields weighted mean

$^{206}Pb/^{238}U$ age of ~252.5 ± 6.9 Ma (mean square of the weighted deviation (MSWD = 0.053) (Fig. 4b, e). These two age groups are close to the Late Proterozoic magmatic event of the Yangtze basement and the ELIP magmatic event of the middle-upper Permian, respectively.

Shangcang rhyolite

The analyzed zircons from the rhyolite are clear, euhedral and have oscillatory zoning patterns either mantling a rounded darker core or shaping a whole zircon crystal (Fig. 4b). These morphological characteristics suggest that the zircon crystals were derived from an igneous origin. This is further reflected by their high Th/U ratios (0.44–0.63). The age of the zircons was calculated based on their $^{206}Pb/^{238}U$ ratios. Of all the tested zircon grains, one sample [Spot DL-32(3)-12] was excluded because it is apparently older than the others, which indicates a probable inherited origin. The rest of the spot ages form a compact cluster on the $^{206}Pb/^{238}U$–$^{207}Pb/^{235}U$ concordia diagram (Fig. 4d). The $^{206}Pb/^{238}U$ ages of the valid zircons ranged from 245.1 ± 5.5 to 263.9 ± 6.8 Ma and yielded a weighted mean age of 252.6 ± 2.2 Ma (MSWD = 1.3) (Fig. 4d). As the zircons have an igneous origin, we interpret this weighted mean age as the formation age of the rhyolite.

Major and trace elements

Major elements

The Wase granite samples both have very high SiO_2 contents (76–80 wt%), but relatively low FeO* (0.13–0.23 wt%) and MgO (0.2–0. wt%) concentrations (Table 3). These characteristics are consistent with their mineral assemblage that shows an overwhelming enrichment in quartz and feldspar while mafic phases are distinctively lacking (Fig. 3d, e). The SiO_2 content of the Shangcang rhyolite are generally lower (~70 to 71 wt%) than the Wase granite (Table 3). The MgO content displays no distinctive difference compared with the granite. Its FeO* (FeO* = 0.7–4.4 wt%) (Table 3), however, is generally higher than in the Wase granite. This feature is consistent with the petrography of the rhyolite that shows significant Fe–Ti oxides within the rhyolitic matrix (Fig. 3f). We use the classification scheme of Frost et al. (2001) to reveal the basic characteristics of the Wase granite and the Shangcang rhyolite. In these diagrams, all the rhyolite samples plot in the ferroan and alkalic area, but the Wase granite samples are magnesian and range from alkali–calcic to calc–alkalic. The ASI ratio [molar Al/(Ca-1.67P+Na+K)] and A/NK ratio [molar $Al_2O_3/(Na_2O+K_2O)$] of the Wase granite samples are both greater than 1; as a result, they plot in the peraluminous quadrant of the diagram (Fig. 5). The ratios

Table 4 Results of the Sr–Nd isotopic analysis of the Wase pluton and Shangcang rhyolite

Sample	Location	Lithology	Rb (ppm)	Sr (ppm)	$^{87}Rb/^{86}Sr$	$^{87}Sr/^{86}Sr$	Error (2σ)	$^{87}Sr/^{86}Sr_{(i)}$	Sm (ppm)	Nd (ppm)	$^{147}Sm/^{144}Nd$	$^{143}Nd/^{144}Nd$	Error (2σ)	$(^{143}Nd/^{144}Nd)_i$	$\varepsilon(Nd)_{(i)}$
DL-07	Wase	Granite	86.9	61.5	4.092	0.730649	0.000007	0.7159 (t = 253 Ma)	1.51	6.85	0.133	0.51191	0.000014	0.5117 (t = 253 Ma)	−12.15 (t = 253 Ma)
HD-15	Wase	Granite	109	118	2.675	0.727892	0.000013	0.7183 (t = 253 Ma)	1.23	5.38	0.138	0.511839	0.000014	0.5116 (t = 253 Ma)	−13.70 (t = 253 Ma)
DL-32(3)	Shangcang	Rhyolite	127	39.4	9.334	0.73885	0.000012	0.7053 (t = 253 Ma)	24.9	128	0.118	0.512498	0.000011	0.5123 (t = 253 Ma)	−0.18 (t = 253 Ma)

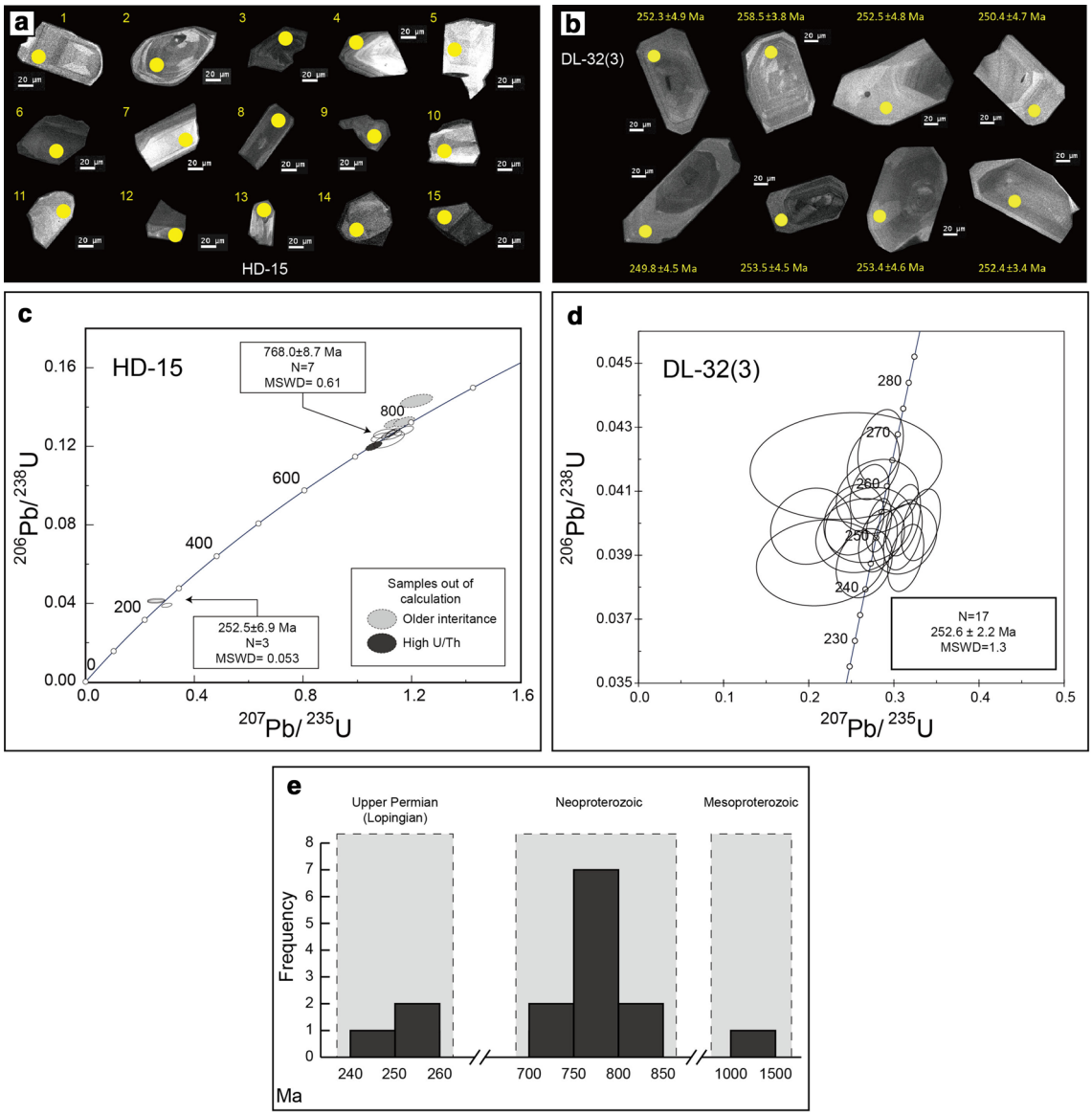

Fig. 4 Results of SHRIMP U–Pb zircon analysis of the Wase pluton (HD-15) and Shangcang rhyolite [DL-32(3)]; **a** CL images of the 15 tested zircon grains of HD-15; **b** CL images of the 15 tested zircon grains of DL-32(3); **c** U–Pb concordia plot for HD-15 zircons; **d** U–Pb concordia plot for DL-32(3) zircons; **e** frequency distribution of zircon ages for HD-15 annotated with the geological time intervals

of the Shangcang rhyolite samples, however, are more variable covering a range from slightly metaluminous to peraluminous (Fig. 5).

Trace elements

Concentrations of rare earth elements (REEs) in the Wase pluton are significantly lower than the Shangcang rhyolite (Table 3; Fig. 6a). The Wase pluton is characterized by a distinctive enrichment of light REEs (LREEs) relative to the heavy REEs (HREEs) (La_N/Yb_N = 6.9–7.1), enrichment of LREEs over middle REEs (MREEs) (La_N/Sm_N = 3.7–4.0) and relatively flat MREE-HREE patterns (Gd_N/Yb_N = 0.93–1.01). The Wase granite samples do not show a distinct Eu anomaly (either positive or negative: Eu/Eu* = 0.74–1.07) (Fig. 6a). For the Shangcang rhyolite, the enrichment of LREEs is greater than the granite, as reflected by the greater La_N/Yb_N ratio (10.5–12.8). Its LREE fractionation is generally similar (La_N/Sm_N = 3.9–4.2) to the granite, whereas its MREE-HREE pattern is slightly inclined (Gd_N/Yb_N = 1.7–1.9). The rhyolite shows a significant negative Eu anomaly (Eu/Eu* = ~0.3). In the primitive mantle-normalized diagram (Fig. 6b), the Wase pluton shows a distinct negative depletion in Nb–Ta and slight enrichment in U, Zr and Hf. In detail, HD-15 shows a slight depletion in Cs and DL-07

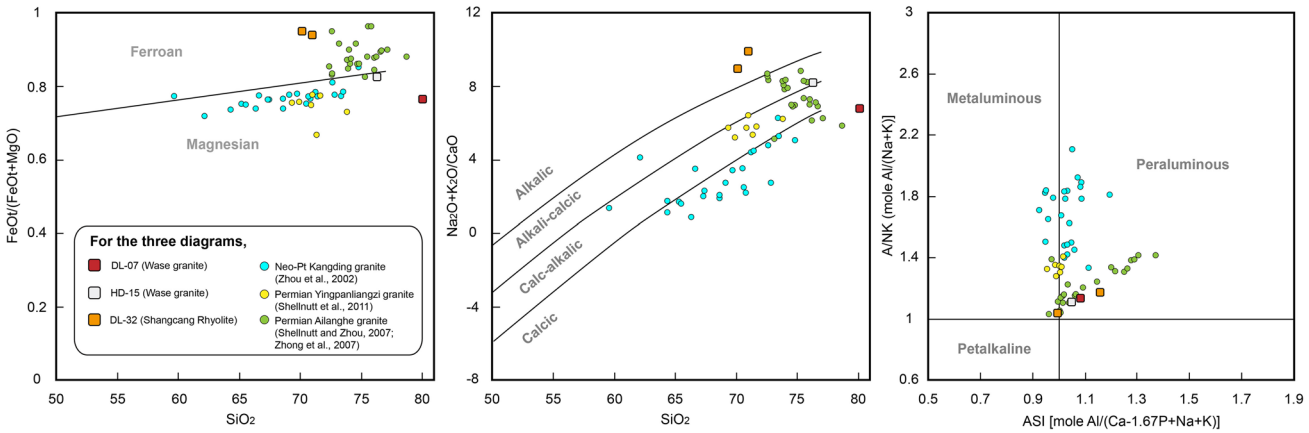

Fig. 5 The classification diagram of Frost et al. (2001). The Yangtze Basement samples are from the Neoproterozoic Kangding granite complex (Zhou et al. 2002). Samples derived from differentiation of mafic magma are from Shellnutt and Zhou (2007). Data for crustally derived granites are from the Ailanghe pluton (Zhong et al. 2007) and the Yingpanliangzi pluton (Shellnutt et al. 2011a, b)

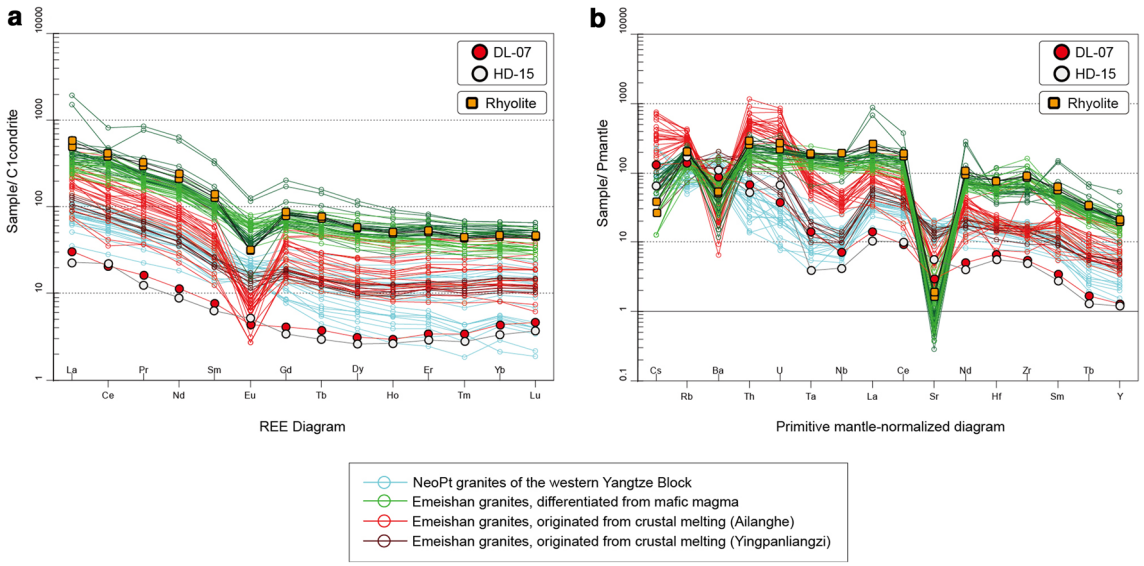

Fig. 6 **a** Chondrite-normalized REE plot (normalizing values from Sun and McDonough 1989) and **b** primitive-mantle-normalized trace element plot (normalizing values from Boynton 1984) for the Wase pluton and Shangcang rhyolite. Other sample suites are plotted for comparison: Yangtze Basement samples (*cyan*) from the Neoproterozoic Kangding granite complex (Zhou et al. 2002); silicic samples derived from differentiation of mafic magma (*green*) from the Baima and Panzhihua plutons (Shellnutt and Zhou 2007); crustally derived granites from the Ailanghe (*dark red*) pluton (Zhong et al. 2007) and the Yingpanliangzi (*light red*) pluton (Shellnutt et al. 2011)

shows a slight depletion in Sr, while the Shangcang rhyolite exhibits a clear depletion in Cs, Ba and Sr.

Sr–Nd isotopes

Initial $^{87}Sr/^{86}Sr_{(i)}$ and $\varepsilon(Nd)_{(i)}$ values for the samples were calculated using the weighted mean age of the younger $^{206}Pb/^{238}U$ age group ($t = 253$ Ma) for the Wase granite and the weighted mean $^{206}Pb/^{238}U$ age ($t = 253$ Ma) for the Shangcang rhyolite. The $^{87}Sr/^{86}Sr_{(t=253\ Ma)}$ values of the Wase granite samples are 0.7159 for DL-07 and 0.7183 for HD-15, whereas the $^{87}Sr/^{86}Sr_{(t=253\ Ma)}$ of the Shangcang rhyolite [DL-32(3)] gives a lower value of 0.7053. The two granite samples show negative $\varepsilon(Nd)_{(t=253\ Ma)}$ values of −12.15 (DL-07) and −13.70 (HD-15), whereas the rhyolite sample [DL-32(3)] is just slightly negative, at −0.18. The $^{87}Sr/^{86}Sr_{(i)}$ versus $\varepsilon(Nd)_{(i)}$ diagram is presented in Fig. 7.

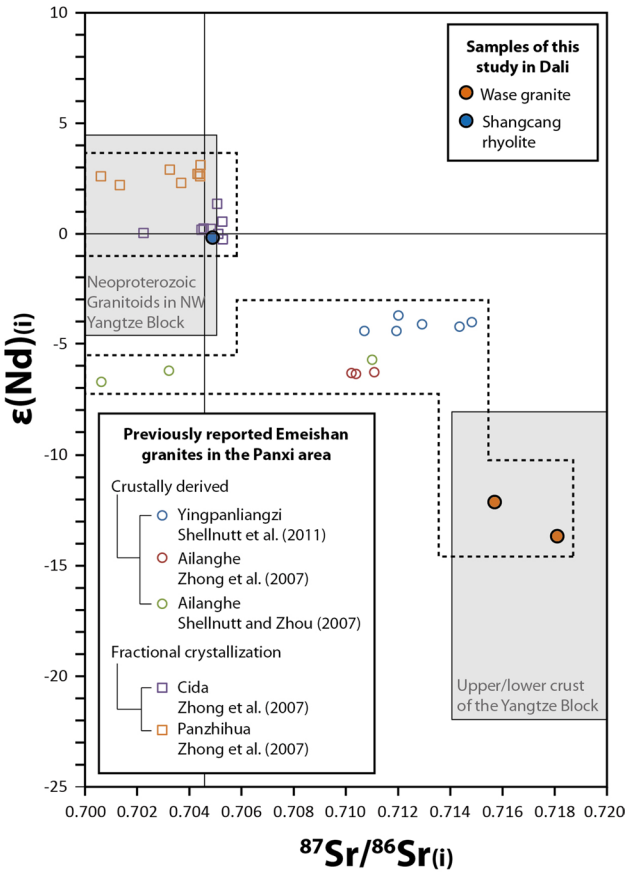

Fig. 7 $^{87}Sr/^{86}Sr_{(i)}$ vs. $\varepsilon(Nd)_{(i)}$ diagram showing how data for the Wase pluton and Shangcang rhyolite compare with other published data on Emeishan granites. The range for the Neoproterozoic granites and Upper Yangtze Block is from Shellnutt et al. (2011)

Discussion

Age of the Wase pluton: Proterozoic or Permian?

The analyzed zircon grains of the Wase pluton form two distinctive age groups on the concordia diagram. One group falls in the Precambrian interval (~768.0 ± 8.7 Ma), which is very close to the age of the Late Neoproterozoic magmatic event of the Yangtze Block (Chen and Jahn 1998; Zhou et al. 2002; Sun et al. 2009; Wang et al. 2012; Lan et al. 2015). The other group, only represented by three grains, has a weighted mean age (~252.5 ± 6.9 Ma) that is very close to the age of the identified Emeishan silicic rocks, including the Shangcang rhyolite (252.6 ± 2.2 Ma) and other silicic plutons reported in the Panxi area, for example, the Aihanghe and the Yingpanliangzi plutons (Zhong et al. 2007; Shellnutt et al. 2011a) (Table 1). As the Wase granite is fresh (LOI < 1) and there is no evidence for obvious Pb loss in its zircon U–Pb system, we interpret the middle Permian age as its formation age. The zircons showing Late Proterozoic ages are probably older grains that were inherited from the Precambrian crust of the Yangtze Block. As mentioned in Shellnutt et al. (2015), several parameters determine whether inherited zircon grains can survive in the new melt (Watson et al. 1996). One of them is the size of the zircon crystals. Zircons with sizes less than 50 µm cannot be preserved at ~700 °C (Shellnutt et al. 2015). Zircons in the Wase pluton that preserve Neoproterozoic ages are mostly smaller than 50 µm, suggesting a melt temperature of <700 °C, which matches the peraluminous nature of the Wase pluton and its lack of melanosome minerals. This inheritance model is consistent with the geological relationship between the Wase pluton and adjacent sedimentary strata (see below) and can be further demonstrated by the trace element and Sr–Nd isotopic features (see "Petrogenetic interpretation").

Geological observations are consistent with an origin for the Wase pluton as part of the Emeishan magmatic event. The lithological contact between the Wase pluton and the Devonian strata obliquely intersects the primary bedding plane of the Devonian limestone strata, clearly precluding the contact being an erosional unconformity between the Yangtze basement and the Paleozoic sedimentary cover. The contact between the Wase pluton and the Devonian strata can potentially be interpreted either as a fault plane or as an intrusive boundary. However, the Devonian limestone strata close to the contact surface have developed a clear metamorphosed marble zone and the primary textures of the layers are totally eliminated in the marbles. Furthermore, there are also no secondary filling materials developed inside the contact region. These observations preclude a fault relationship and the only reasonable interpretation of the lithological contact is that it is an intrusive boundary. These geological implications support the ~253 Ma ages of the younger zircons as representing the time of formation of the Wase granite. However, only three zircon grains have ~253 Ma ages, which limits the precision of the weighted mean (±6 Ma). Furthermore, Shellnutt et al. (2012) re-analyzed some Panxi paleo-rift plutons using the CA-TIMS method and showed that the SHRIMP ages were systematically offset to younger ages (by ~7 Myrs) compared to the CA-TIMS due to issues with the SHRIMP calibration standards. Therefore, we conclude that the Wase pluton is definitely part of the ELIP event, but its absolute age is somewhat uncertain.

Petrogenetic interpretation

Formation mechanism and origin of the Wase granite

The dominant zircon population ($N = 7$) displays a weighted mean age of ~768.0 ± 8.7 Ma, consistent with the age of the Neoproterozoic magmatism of the Yangtze

block (Chen and Jahn 1998; Zhou et al. 2002; Sun et al. 2009; Wang et al. 2012; Lan et al. 2015). As mentioned above, the Wase pluton is related to the ELIP event, so these older zircon grains are probably inherited from re-melted crustal materials that were originally produced by the Late Neoproterozoic magmatism (Watson 1996; Shellnutt et al. 2015). Numerous magmatic events have been recorded in the Precambrian history of the Yangtze block since it was developed from an Archaean crystalline basement (Sun et al. 2009). The Neoproterozoic magmatism is the latest episode recorded in the Precambrian Yangtze Block, which was then succeeded by development of a sedimentary cover from Sinian to Phanerozoic times (Sun et al. 2009; Wang et al. 2012; Lan et al. 2015). Geological systems related to this magmatic event include the original plutonic rocks (e.g. the Kangding granitic complex) that intruded into the Pre-Neoproterozoic metamorphic complexes (Ling et al. 2001; Zhou et al. 2002) and the initial sedimentary cover of the Yangtze Block that was potentially eroded from the igneous rocks, for example, the Liantuo Formation (e.g. Lan et al. 2015), the Chengjiang Formation (e.g. Wang et al. 2012), the Lieguliu formation and Guanyinya Formation (Sun et al. 2009), which contain detrital zircons or tuffaceous interlayers that record a youngest age of ~700 to 800 Ma. These units are highly evolved crustal materials enriched in aluminum. They can be regarded as representative of the typical upper crust of the Upper Yangtze Block.

The negative $\varepsilon(Nd)_{(i)}$ (−12.2 and −13.7) and high $^{87}Sr/^{86}Sr_{(i)}$ values (0.7159 and 0.7183) of the Wase Granite are indicative of a highly-evolved upper crustal source. In the Sr–Nd isotopic diagram, the $^{87}Sr/^{86}Sr_{(i)}$ and $\varepsilon(Nd)_{(i)}$ value of the Wase granite plot was within the range of the upper crust of the Yangtze Block (Fig. 7, the Yangtze crust area after Shellnutt et al. 2011a). This is consistent with the inheritance of Neoproterozoic-aged zircon grains as discussed above. In the primitive-mantle-normalized diagram (Fig. 6b), the Wase pluton samples exhibit depletions in Nb, Ta and enrichments in Pb, U, consistent with a crustally derived origin, while the REE diagram shows enrichment of LREE over HREE (La_N/Yb_N = 6.91–7.07) with no significant Eu anomaly (Eu/Eu* = 0.74–1.07) (Fig. 6a), suggesting the primary magma of the Wase pluton did not experience feldspar fractionation or did not form from partial melting of a feldspar-rich cumulate source (Zhong et al. 2007; Shellnutt et al. 2011a). The relatively flat HREE pattern in the REE diagram of the Wase granite (Gd_N/Yb_N = 0.93–1.01) implies that its magma source did not contain residual garnet which can sequester the HREEs (Shellnutt et al. 2011a) (Fig. 6a). The peraluminous nature of the Wase pluton indicates it was derived from a Si–Al enriched source (Fig. 5). Supported by these observations, the parent magma of the Wase pluton is unlikely to be formed in lower crust but rather derived from a middle-upper crust level, thus being consistent with its Sr–Nd isotope features and inherited zircon ages. These characteristics correspond with the other (and the only two currently known) cases of crustally derived granites of the ELIP, i.e. the Yingpanliangzi and the Ailanghe plutons (Zhong et al. 2007; Shellnutt et al. 2011a) (Fig. 6).

As the Wase pluton is the first example of a crustally derived granite located outside the Panxi area, it can be inferred that melting of the Yangtze basement during the ELIP event was not a localized phenomenon confined to the Panxi paleo-rift, but rather a more widespread mechanism that occurred in a wider region around the plume axis (i.e. the Central ELIP). The ELIP-related silicic rocks developed in Northern Vietnam (Phan Si Pan uplift) which are inferred to have been produced in the Central ELIP but later dislocated by the Red River-Ailaoshan fault, also support this conclusion (Tran et al. 2015; Usuki et al. 2015). This implies that the Yangtze Block perhaps underwent a significant rejuvenation stage during the middle-late Permian under the effect of the Emeishan mantle plume.

Comparison between the Shangcang rhyolite and Wase granite

As the Wase pluton and the Shangcang rhyolite share a very similar formation age (~253 Ma) and are spatially adjacent (Figs. 1c, 2), the question is whether there is any genetic links between them. As shown in Fig. 7, the Shangcang rhyolite exhibit a moderate $^{87}Sr/^{86}Sr_{(i)}$ value (0.7053) and a slightly negative $\varepsilon(Nd)_{(i)}$ value (−0.18), which plot in range of mantle-derived felsic plutons of the Panxi area (e.g. Cida and Taihe) (Shellnutt and Zhou 2007). This observation indicates that the rhyolite was derived from a mantle-derived source and unlikely to be formed by crustal melting. In the REE diagram and primitive-mantle-normalized diagram (Fig. 6), the Shangcang rhyolite samples show similar patterns to the Taihe, Panzhihua and Baima plutons (Shellnutt and Zhou 2007; Shellnutt et al. 2009) that are characterized by strong negative Eu anomalies and depletions in Cs, Ba and Sr, implying the parent magma of the rhyolite is derived from a differentiated magma after significant fractional crystallization of feldspar, but unlikely to be formed by partial melting of the fractionated feldspar cumulates. These characteristics are different from the Wase pluton, suggesting there are no genetic links between the sources of these two silicic systems, despite their close temporal, spatial and stratigraphical relationships. On the other hand, the existence of highly heterogeneous silicic systems developed in the same place, as the thickest volcanic

pile that contains picrites (e.g. Xu et al. 2001), proximal volcaniclastic facies (Zhu et al. 2014) and is frequently cross-cut by dikes (Zhu et al. 2014; Li et al. 2015), implies that the Dali area is probably a location where the most robust activities of the Central ELIP magmatism occurred.

Thermodynamics modeling

After inferring the source and formation mechanism of the Wase granite and Shangcang rhyolite, we use thermodynamic modeling to understand further details on their petrogenesis. For the Wase granite, the question is if it can be theoretically produced from real compositions of the Yangtze upper crust, as predicted from its geochemical and isotope characters. For the Shangcang rhyolite, which is suggested as differentiated from mafic magma, the point is if typical Emeishan basaltic magma can generate silicic melts similar to the Shangcang rhyolite. For the modelling, we used Rhyolite-MELTs (Gualda et al. 2012; Gualda and Ghiroso 2015) as this software has been used effectively in previous petrogenetic studies of the ELIP (e.g. Shellnutt et al. 2011b, 2015; Shellnutt and Iizuka 2012; Tran et al. 2015).

Wase granite

The modeling parameters for the Wase granite must factor into consideration the source composition, starting temperature, pressure, initial water content and relative oxidation state. The Wase granite contains abundant inherited Neoproterozoic zircon grains, which is helpful for tracing the possible source. In the western margin of the Yangtze Block, a series of Neoproterozoic igneous rock were recognized (e.g. Ling et al. 2001). The age, spatial location, geochemical features and tectonic background of the Neoproterozoic granitoids suggest that they may be the most plausible source of the Wase granite. We selected the composition of Sample-3, Huangcaoshan granite (788 ± 11 Ma, Ling et al. 2001) as the starting composition (Table 5). As Neoproterozoic materials in the western Yangtze block were estimated to have been buried to a depth of ~10 km (Deng et al. 2016), we ran the model at 3 kbar pressure. The oxygen fugacity was set to FMQ-1, based on the estimation of oxidized area range in the Central ELIP (Shellnutt and Iizuka 2012). The starting temperature was set to 1300 °C, according to the temperature of the heat source—mafic magma. The initial water content was set to 0.5 wt% because the Wase granite does not contain hydrous minerals (Table 5).

The modeling results are depicted in Fig. 8 and the original dataset is in our supplementary material (Table S1). The curves show the evolution of melt compositions as temperature decreases under isobaric conditions. As seen in these charts, felsic elements (K_2O, Na_2O, Al_2O_3, CaO, P_2O_5) of the Wase granite are mostly consistent with the melt evolution trend, whereas mafic elements (MgO, FeOt and TiO_2) generally plot below the curves. We interpret the discrepancies of MgO, FeOt and TiO_2 as caused by crystallization and removal of mafic and Fe–Ti minerals during ascent of the melt. Therefore, we think it is reasonable to conclude that re-melted upper Yangtze crust can produce compositions similar to that of Wase granite.

Table 5 Starting parameter sets of MELTs modeling

Compositions (wt%)	Sample-3, Huangcaoshan Granite	WL12, Shangcang ELIP Basalt
SiO_2	77.42	57.86
TiO_2	0.11	3.91
Al_2O_3	11.32	10.8
Fe_2O_3	0.70	1.78
FeO	0.40	9.1
MnO	0.03	0.13
MgO	0.35	2.54
CaO	0.56	10.33
Na_2O	3.66	1.07
K_2O	4.62	0.08
P_2O_5	0.11	0.43
H_2O	0.5	0.1
fO_2	FMQ-1	FMQ-1
Pressure	3 kbar	1.2 kbar
Data from	Ling et al. (2001a, b)	Xiao et al. (2004)

Shangcang rhyolite

The Shangcang rhyolite is thought to be derived by fractional crystallization of parental magma similar in composition to Emeishan flood basalt. Flood basalts in the Central ELIP erupted in a relatively short time interval, so it is reasonable to regard some of them as undifferentiated mafic magma. In the Shangcang section, over 4000 m basalt erupted before the rhyolite (Fig. 2). Based on Ti/Y ratios, these basalts were divided into two major groups (low-Ti, high-Ti), representing two different mantle sources (Xu et al. 2001; Xiao et al. 2004). For the modeling, it is necessary to find an appropriate starting composition from these diverse magma types. As the ratios of some trace elements (e.g. Nb/Yb and Th/Yb) do not change significantly with magma evolution (Pearce and Peate 1995), they are useful to trace the potential correlation between the mafic and silicic lithology. Figure 9 shows that the high-Ti and low-Ti basalts can be distinguished by their Nb/Yb and Th/

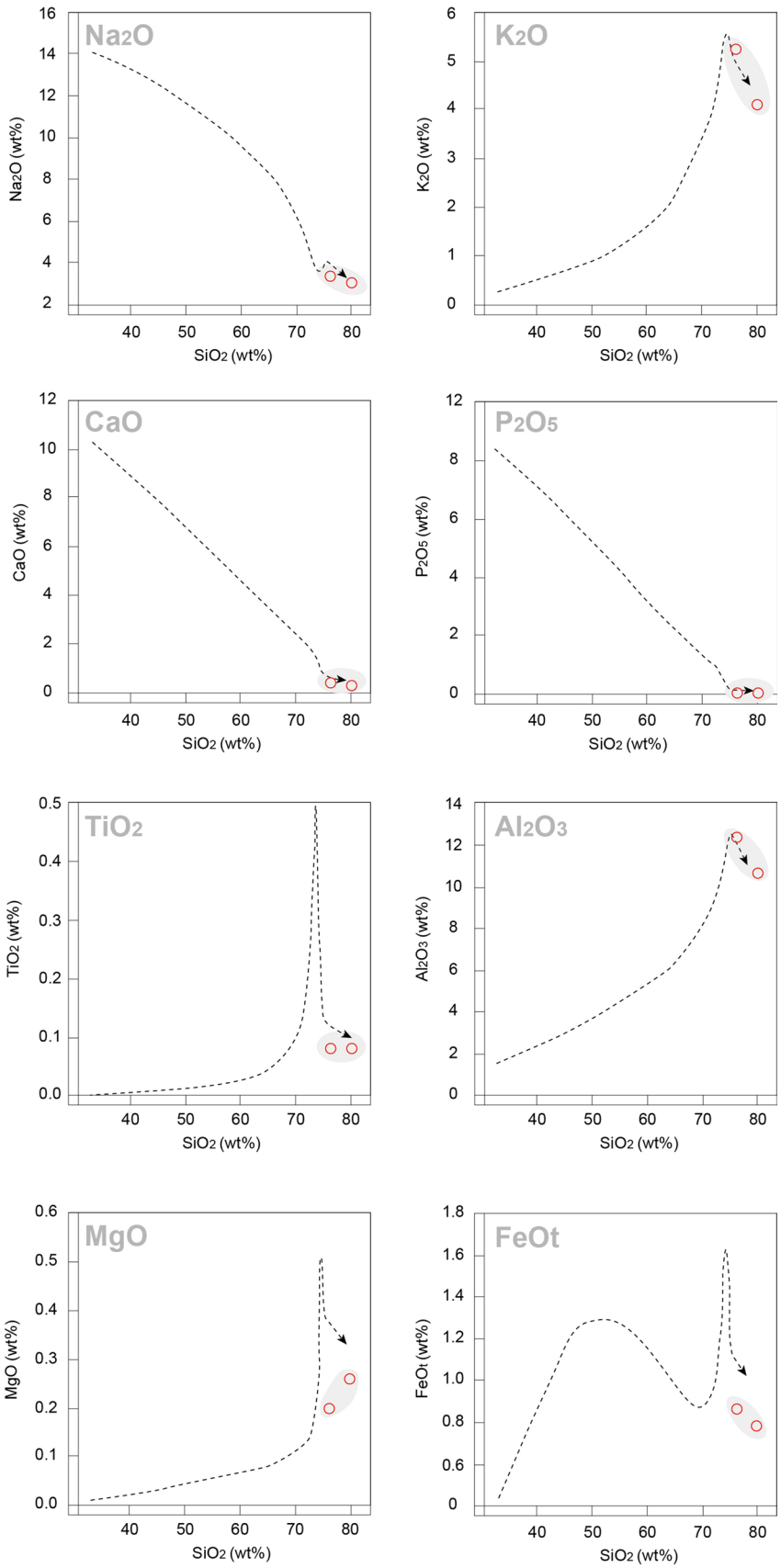

Fig. 8 MELTs modeling results of the Wase granite. The *red circles* represent the compositions of HD-15 and DL-07. The *dashed curves* represent the calculated melt evolution trend as temperature decreases from 1300 °C: the *arrow* indicates direction of decreasing temperature

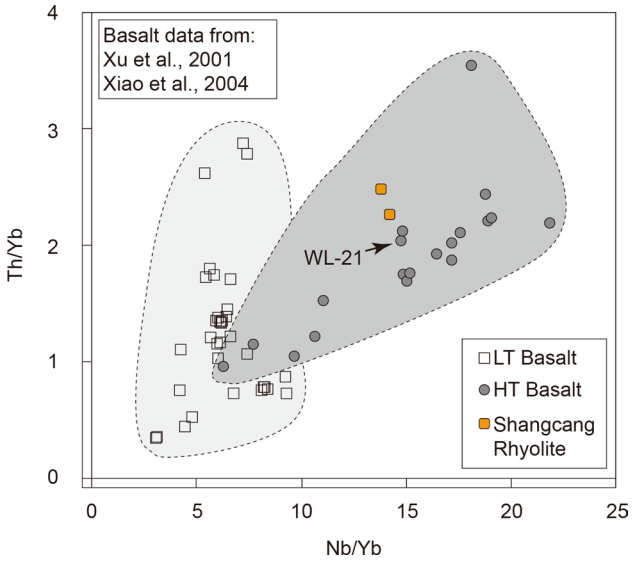

Fig. 9 Nb/Yb vs. Th/Yb diagram (Pearce and Peate 1995) of Emeishan basalts and rhyolites in the Shangcang section. The values of Emeishan basalts are referred to from Xu et al. (2001) and Xiao et al. (2004)

Yb ratios, and the Shangcang rhyolite plots with the high-Ti group. Therefore, we chose WL-12, a high-Ti basalt sample from Xiao et al. (2004), as the starting composition (Table 5). The model was run with an initial temperature of 1300 °C, a pressure of 1.2 kbar (~4 km), an oxidation state at FMQ-1 and an initial water content of 0.1 wt% (Table 5).

The modeling results are presented in Fig. 10 and the original data are listed in supplementary Table S2. Some major elements (FeOt, MgO, TiO_2 and Al_2O_3) are consistent with the melt evolution curve. Alkali elements (Na_2O and K_2O) show obvious enrichment, whereas CaO and P_2O_5 are depleted compared with the modeling end point. We interpret the depletion of CaO and P_2O_5 as caused by apatite crystallization during ascent of the rhyolitic magma. The enrichment of alkali elements is perhaps due to post-eruption alteration from plagioclase to alkali feldspar. In order to check whether apatite crystallization and alteration of plagioclase can be reasonable interpretations for the modeling result, we introduce a new parameter 'Pl_{tot}' to refer to the overall values of CaO and Na_2O finally preserved in the Shangcang rhyolite plus the values of CaO consumed during apatite crystallization:

$$Pl_{tot} = CaO_{rhy} + (P_2O_{5model} - P_2O_{5rhy})42.06/55.38 + Na_2O_{rhy},$$

where the formula P_2O_{5model} refers to the P_2O_5 value at the end point of the modeled melt evolution curve. CaO_{rhy}, P_2O_{5rhy} and Na_2O_{rhy} are measured rhyolite values from our whole-rock geochemical data. We plot Pl_{tot} into a SiO_2 vs. ($CaO+Na_2O$) diagram. The parameter points are in agreement with the melt evolution curve of modeling sums of CaO and Na_2O. This result demonstrates that apatite crystallization and alteration of Ca-rich plagioclase to Na-rich plagioclase is a plausible interpretation for the discrepancy (Figs. 11, 12). Xu et al. (2010) also argued that the silicic magmas in Shangcang were probably contaminated by continental materials, resulting in a lower trend of the $^{87}Sr/^{86}Sr_{(i)}$ and $\varepsilon(Nd)_{(i)}$ characteristics compared with the range of Emeishan basalts. This may also explain the high value of K_2O (as well as some Na_2O) compared with the modeled melt evolution curve.

Conclusion

A new granite pluton (the Wase pluton) was found in the Wase town of the Dali area, which is one of the principal exposed areas of volcanics in the central Emeishan Large Igneous Province (ELIP). This pluton is less affected by tectonic activity and is closely related to the thickest Emeishan volcanic sequence (the Shangcang section) in the whole ELIP. By analyzing its geological relationships, SHRIMP U–Pb age, geochemical and isotopic features, we interpret this pluton as formed during the ELIP flood volcanic event. Its magma source is derived from re-melting of upper crust materials of the Yangtze Block, probably by the heat from mafic intrusions related to the Emeishan mantle plume activity. Three types of evidence support the following conclusion:

1. Geologically, the orientation of the boundary contact between the Wase pluton and surrounding Devonian limestone strata shows oblique intersection with the primary bedding of the limestone strata. The carbonate materials immediately in contact with the granite have been metamorphosed to marble. These observations indicate that this lithological boundary is an intrusive contact and thus constrains the formation of the granite to after the deposition of the Devonian strata.
2. Chronologically, the Wase pluton contains two distinct groups of SHRIMP zircon U–Pb ages. One group has a Late Neoproterozoic age of ~768 Ma, close to the age of the Neoproterozoic magmatism recorded in the basement of the Yangtze Block, while the other group (~253 Ma) is consistent with the Permian ELIP magmatism. Constrained by the geological relationship, the Permian age can be assured as the formation age of the Wase pluton, whereas the Proterozoic-aged zircon grains were likely inherited from products of the Neoproterozoic magmatism of the Yangtze Block, implying a crustally derived magma origin.

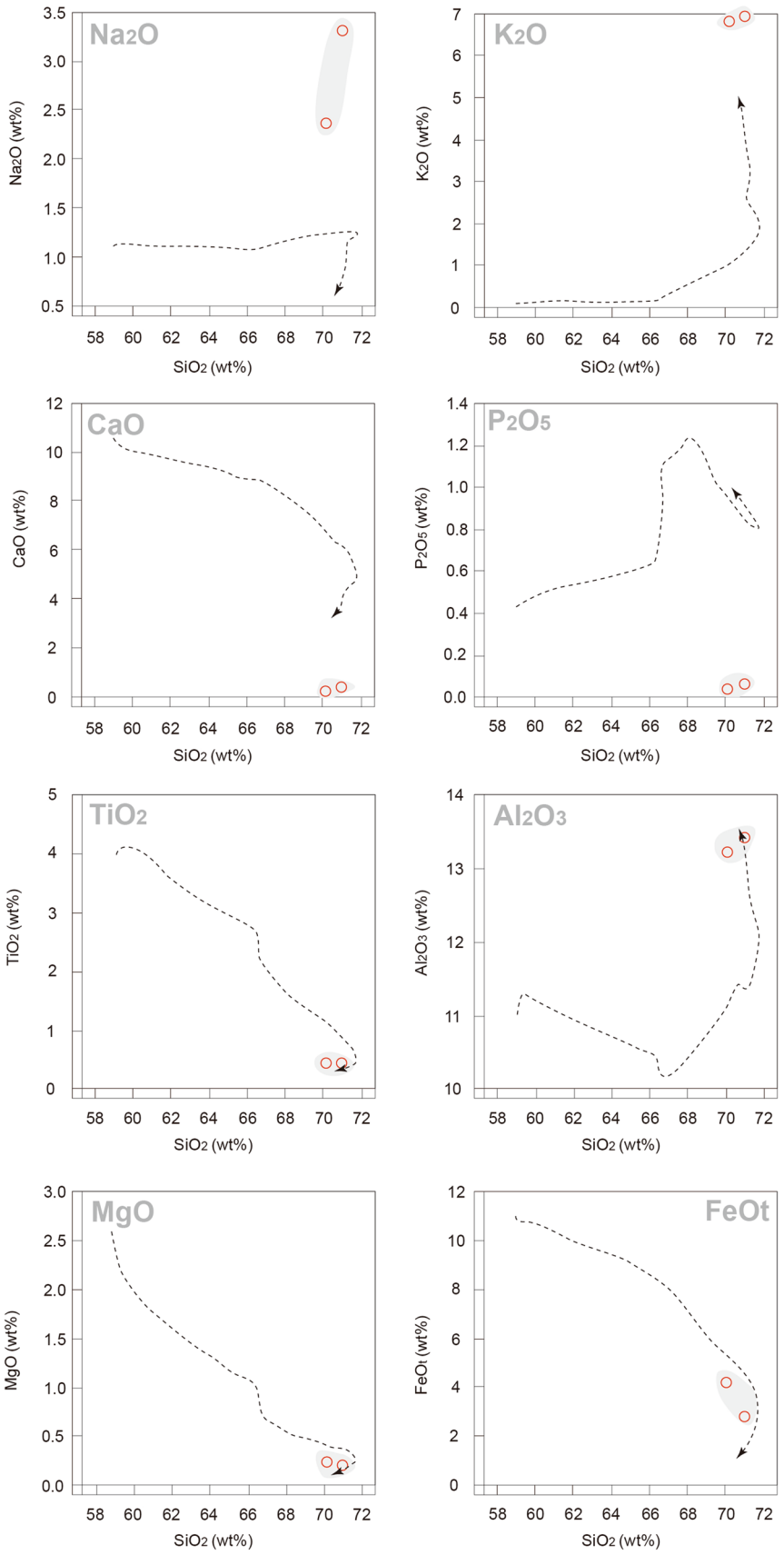

Fig. 10 MELTs modeling results of the Shangcang rhyolite. The *red circles* represent the composition of DL-32. The *dashed curves* represent the calculated melt evolution trend as temperature decreases from 1300 °C: the *arrow* indicates direction of decreasing temperature

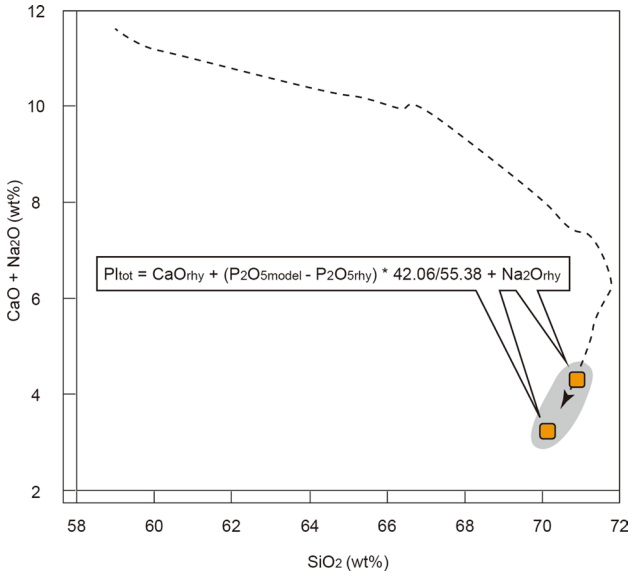

Fig. 11 The Pl_{tot} parameters of the Shangcang rhyolite are plotted with the MELTs evolving curve of $CaO+Na_2O$, indicating apatite crystallization and alteration of plagioclase may be a reasonable interpretation for the results

3. Geochemically, the Wase pluton is peraluminous and displays negative Nb–Ta anomalies, enrichment in U, Th and LREE, high $^{87}Sr/^{86}Sr_{(i)}$ value and strongly negative $\varepsilon(Nd)_{(i)}$ values, consistent with a crustally derived magma source. It also shows no obvious Eu anomaly (either positive or negative), precluding a derivation from fractional crystallization of mantle-derived mafic magma or through partial melting of feldspar-rich cumulates.

Although the age of the Wase pluton is similar to that of the rhyolite found in the uppermost level of the local ELIP sequence, they are unlikely to be generated from the same magma source. This is because the rhyolite has relatively lower $^{87}Sr/^{86}Sr_{(i)}$ ratio, slightly negative $\varepsilon(Nd)_{(i)}$ values and exhibits negative anomalies in Eu, Cs, Ba, Sr, which are obviously different from the Wase granite. These characteristics demonstrate that the rhyolite is probably generated by fractional crystallization of a mantle-derived mafic magma. The co-existence of both crustally derived and mantle-derived felsic units and their spatial association with diabase dike swarms, vent-proximal volcanics and the thickest flood basalt piles in the ELIP imply that the Dali area

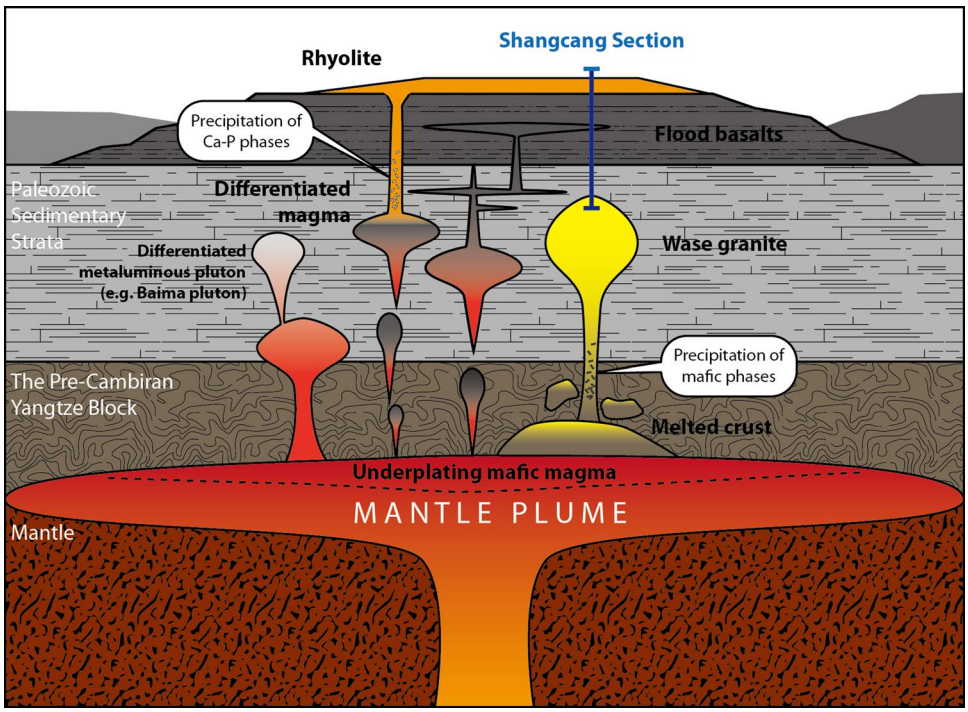

Fig. 12 A cartoon model summarizing the petrogenetic origin of the Wase pluton and the Shangcang rhyolite (not to scale). A representative metaluminous pluton of the Panxi area (e.g. Baima) is also shown to show the diversity (Shellnutt et al. 2009)

is probably the location where the most robust magmatism once existed during the Permian ELIP event.

Acknowledgements Zhaojie Guo was supported financially by the Natural Science Foundation of China (No. 41572199) and Bei Zhu by Young Scholars Development Fund of Southwest Petroleum University (No. 201699010090). We thank Dr. Ingrid Ukstins Peate for valuable discussions during this study. We thank Prof. J. Gregory Shellnutt for his review and constructive comments and thank Wolf-Christian Dullo and Ingo Braun, editors of the International Journal of Earth Sciences, for their valuable editorial suggestions.

References

Ali JR, Thompson GM, Zhou MF, Song X (2005) Emeishan large igneous province, SW China. Lithos 79(3):475–489. doi:10.1016/j.lithos.2004.09.013

Anh TV, Pang K-N, Chung S-L, Lin H-M, Hoa TT, Anh TT, Yang H-J (2011) The Song Da magmatic suite revisited: a petrologic, geochemical and Sr–Nd isotopic study on picrites, flood basalts and silicic volcanic rocks. J Asian Earth Sci 42(6):1341–1355. doi:10.1093/petrology/42.11.2033

Black LP, Kamo SL, Allen CM, Aleinikoff JN, Davis DW, Korsch RJ, Foudoulis C (2003) TEMORA 1: a new zircon standard for Phanerozoic U–Pb geochronology. Chem Geol 200(1):155–170. doi:10.1016/s0009-2541(03)00165-7

Boynton WV (1984) Cosmochemistry of the rare earth elements: meteorite studies. In: Rare earth element geochemistry, pp 63–114. doi:10.1016/b978-0-444-42148-7.50008-3

Bryan SE, Ernst RE (2008) Revised definition of large igneous provinces (LIPs). Earth Sci Rev 86(1):175–202. doi:10.1016/j.earscirev.2007.08.008

Bryan SE, Peate IU, Peate DW, Self S, Jerram DA, Mawby MR, Marsh J, Miller JA (2010) The largest volcanic eruptions on Earth. Earth Sci Rev 102(3):207–229. doi:10.1016/j.earscirev.2010.07.001

Campbell IH (2005) Large igneous provinces and the mantle plume hypothesis. Elements 1(5):265–269. doi:10.2113/gselements.1.5.265

Campbell IH (2007) Testing the plume theory. Chem Geol 241(3):153–176. doi:10.1016/j.chemgeo.2007.01.024

Campbell IH, Griffiths RW (1990) Implications of mantle plume structure for the evolution of flood basalts. Earth Planet Sci Lett 99(1):79–93. doi:10.1016/0012-821x(90)90072-6

Chen J, Jahn BM (1998) Crustal evolution of southeastern China: Nd and Sr isotopic evidence. Tectonophysics 284(1):101–133. doi:10.1016/s0040-1951(97)00186-8

Chung SL, Jahn BM (1995) Plume-lithosphere interaction in generation of the Emeishan flood basalts at the Permian-Triassic boundary. Geology 23(10):889–892. doi:10.1130/0091-7613(1995)023<0889:pliigo>2.3.co;2

Chung SL, Jahn BM, Genyao W, Lo CH, Bolin C (1998) The Emeishan Flood Basalt in SW China: a mantle plume initiation model and its connection with continental breakup and mass extinction at the Permian-Triassic Boundary. In: Flower MFJ, Chung S-L, Lo CH, Lee TY (eds) Mantle dynamics and plate interactions in East Asia. American Geophysical Union Geodynamic Series, vol 27, pp 47–58. doi:10.1029/GD027p0047

Compston W, Williams I, Meyer C (1984) U–Pb geochronology of zircons form lunar Breccia 73217 using a sensitive high mass-resolution ion microprobe. Lunar Planet Sci Conf Proc 89(2):525. doi:10.1029/jb089is02p0b525

Deng Y, Chen Y, Wang P, Essa KS, Xu T, Liang X, Badal J (2016) Magmatic underplating beneath the Emeishan large igneous province (South China) revealed by the COMGRA-ELIP experiment. Tectonophysics 672:16–23. doi:10.1016/j.tecto.2016.01.039

Frost BR, Barnes CG, Collins WJ, Arculus RJ, Ellis DJ, Frost CD (2001) A geochemical classification for granitic rocks. J Petrol 42(11):2033–2048. doi:10.1093/petrology/42.11.2033

Griffiths RW, Campbell IH (1990) Stirring and structure in mantle starting plumes. Earth Planet Sci Lett 99(1):66–78. doi:10.1016/0012-821x(90)90071-5

Griffiths RW, Campbell IH (1991) Interaction of mantle plume heads with the Earth's surface and onset of small-scale convection. J Geophys Res 96(B11):18295–18218, 18310. doi:10.1029/91jb01897

Gualda GA, Ghiorso MS (2015) MELTS_Excel: a Microsoft Excel-based MELTS interface for research and teaching of magma properties and evolution. Geochem Geophys Geosyst 16(1):315–324. doi:10.1002/2014GC005545

Gualda GA, Ghiorso MS, Lemons RV, Carley TL (2012) Rhyolite-MELTS: a modified calibration of MELTS optimized for silica-rich, fluid-bearing magmatic systems. J Petrol 53(5):875–890. doi:10.1093/petrology/egr080

Hanski E, Walker RJ, Huhma H, Polyakov GV, Balykin PA, Tran TH, Ngo TP (2004) Origin of the Permian-Triassic komatiites, northwestern Vietnam. Contrib Miner Petrol 147(4):453–469. doi:10.1007/s00410-004-0567-1

He B, Xu YG, Huang XL, Luo ZY, Shi YR, Yang QJ, Yu SY (2007) Age and duration of the Emeishan flood volcanism, SW China: geochemistry and SHRIMP zircon U–Pb dating of silicic ignimbrites, post-volcanic Xuanwei Formation and clay tuff at the Chaotian section. Earth Planet Sci Lett 255(3):306–323. doi:10.1016/j.epsl.2006.12.021

Jerram DA, Widdowson M, Wignall PB, Sun Y, Lai X, Bond DP, Torsvik TH (2016) Submarine palaeoenvironments during Emeishan flood basalt volcanism, SW China: implications for plume–lithosphere interaction during the Capitanian, Middle Permian ('end Guadalupian') extinction event. Palaeogeogr Palaeoclimatol Palaeoecol 441:65–73. doi:10.1016/j.palaeo.2015.06.009

Lan Z, Li XH, Zhu M, Zhang Q, Li QL (2015) Revisiting the Liantuo Formation in Yangtze Block, South China: SIMS U–Pb zircon age constraints and regional and global significance. Precambrian Res 263:123–141. doi:10.1016/j.precamres.2015.03.012

Li ZX, Li XH, Zhou H, Kinny PD (2002) Grenvillian continental collision in south China: new SHRIMP U–Pb zircon results and implications for the configuration of Rodinia. Geology 30(2):163–166. doi:10.1130/0091-7613(2002)030<0163:gccisc>2.0.co;2

Li ZX, Li XH, Kinny P, Wang J, Zhang S, Zhou H (2003) Geochronology of Neoproterozoic syn-rift magmatism in the Yangtze Craton, South China and correlations with other continents: evidence for a mantle superplume that broke up Rodinia. Precambrian Res 122(1):85–109. doi:10.1016/s0301-9268(02)00208-5

Li XH, Li ZX, Sinclair JA, Li WX, Carter G (2006) Revisiting the "Yanbian Terrane": implications for Neoproterozoic tectonic evolution of the western Yangtze Block, South China. Precambrian Res 151(1):14–30. doi:10.1016/j.precamres.2006.07.009

Li CF, Li XH, Li QL, Guo JH, Li XH (2011) Directly determining 143 Nd/144 Nd isotope ratios using thermal ionization mass spectrometry for geological samples without separation of Sm–Nd. J Anal At Spectrom 26(10):2012–2022. doi:10.1039/c0ja00081g

Li CF, Li XH, Li QL, Guo JH, Li XH, Yang YH (2012) Rapid and precise determination of Sr and Nd isotopic ratios in geological

samples from the same filament loading by thermal ionization mass spectrometry employing a single-step separation scheme. Anal Chim Acta 727:54–60. doi:10.1016/j.aca.2012.03.040

Li H, Zhang Z, Ernst R, Lü L, Santosh M, Zhang D, Cheng Z (2015) Giant radiating mafic dyke swarm of the Emeishan Large Igneous Province: Identifying the mantle plume centre. Terra Nova 27(4):247–257. doi:10.1111/ter.12154

Ling HF, Shen WZ, Wang RC, Xu SJ (2001a) Geochemical characteristics and genesis of Neoproterozoic granitoids in the northwestern margin of the Yangtze Block. Phys Chem Earth Part A 26(9):805–819. doi:10.1016/s1464-1895(01)00129-6

Ling HF, Shen WZ, Wang R-C, Xu SJ (2001b) Geochemical characteristics and genesis of Neoproterozoic granitoids in the northwestern margin of the Yangtze Block. Phys Chem Earth Part A 26(9):805–819. doi:10.1016/s1464-1895(01)00129-6

Ling W, Gao S, Zhang B, Li H, Liu Y, Cheng J (2003) Neoproterozoic tectonic evolution of the northwestern Yangtze craton, South China: implications for amalgamation and break-up of the Rodinia Supercontinent. Precambrian Res 122(1):111–140. doi:10.1016/s0301-9268(02)00222-x

Loiselle M, Wones D (1979) Characteristics and origin of anorogenic granites. In: Geological Society of America Abstracts with Programs, p 468

Ludwig K (2012) Isoplot/Ex, v. 3.75. Berkeley Geochronology Center Special Publication, California, p 5

Luo Z, Xu Y, He B, Shi Y, Huang X (2007) Geochronologic and petrochemical evidence for the genetic link between the Maomaogou nepheline syenites and the Emeishan large igneous province. Chin Sci Bull 52(7):949–958. doi:10.1007/s11434-007-0112-5

Pearce JA and Peate DW (1995) Tectonic implications of the composition of volcanic arc lavas. Annu Rev Earth Planet Sci 23:251–285. doi:10.1146/annurev.ea.23.050195.001343

Peccerillo A, Barberio M, Yirgu G, Ayalew D, Barbieri M, Wu T (2003) Relationships between mafic and peralkaline silicic magmatism in continental rift settings: a petrological, geochemical and isotopic study of the Gedemsa volcano, central Ethiopian rift. J Petrol 44(11):2003–2032. doi:10.1093/petrology/egg068

Regional Stratigraphic Workgroup of Yunnan (RSWY) (1978) Regional stratigraphic chart of the SW China, (Yunnan). Geological Publishing House, Beijing **(in Chinese)**

Shellnutt JG (2014) The Emeishan large igneous province: a synthesis. Geosci Front 5(3):369–394. doi:10.1016/j.gsf.2013.07.003

Shellnutt JG, Iizuka Y (2012) Oxidation zonation within the Emeishan large igneous province: evidence from mantle-derived syenitic plutons. J Asian Earth Sci 54:31–40. doi:10.1016/j.jseaes.2012.03.011

Shellnutt J, Jahn BM (2010) Formation of the Late Permian Panzhihua plutonic-hypabyssal-volcanic igneous complex: implications for the genesis of Fe–Ti oxide deposits and A-type granites of SW China. Earth Planet Sci Lett 289(3):509–519. doi:10.1016/j.epsl.2009.11.044

Shellnutt JG, Zhou MF (2007) Permian peralkaline, peraluminous and metaluminous A-type granites in the Panxi district, SW China: their relationship to the Emeishan mantle plume. Chem Geol 243(3):286–316. doi:10.1016/j.chemgeo.2007.05.022

Shellnutt JG, Zhou MF (2008) Permian, rifting related fayalite syenite in the Panxi region, SW China. Lithos 101(1):54–73. doi:10.1016/j.lithos.2007.07.007

Shellnutt JG, Zhou M-F, Zellmer GF (2009) The role of Fe–Ti oxide crystallization in the formation of A-type granitoids with implications for the Daly gap: an example from the Permian Baima igneous complex, SW China. Chem Geol 259(3):204–217. doi:10.1016/j.chemgeo.2008.10.044

Shellnutt JG, Jahn BM, Zhou MF (2011a) Crustally-derived granites in the Panzhihua region, SW China: implications for felsic magmatism in the Emeishan large igneous province. Lithos 123(1):145–157. doi:10.1016/j.lithos.2010.10.016

Shellnutt JG, Wang K-L, Zellmer GF, Iizuka Y, Jahn B-M, Pang K-N, Qi L, Zhou M-F (2011b) Three Fe-Ti oxide ore-bearing gabbro-granitoid complexes in the Panxi region of the Permian Emeishan large igneous province, SW China. Am J Sci 311(9):773–812. doi:10.2475/09.2011.02

Shellnutt JG, Denyszyn SW, Mundil R (2012) Precise age determination of mafic and felsic intrusive rocks from the Permian Emeishan large igneous province (SW China). Gondwana Res 22(1):118–126. doi:10.1016/j.gr.2011.10.009

Shellnutt JG, Usuki T, Kennedy AK, Chiu H-Y (2015) A lower crust origin of some flood basalts of the Emeishan large igneous province, SW China. J Asian Earth Sci 109:74–85. doi:10.1016/j.jseaes.2015.04.037

Shen WZ, Gao JF, Xu SJ, Tan GQ, Yang ZS, Yang QW (2003) Age and geochemical characteristics of the Lengshuiqing body in the Yanbian region, Sichuan Province. Acta Petrol Sin 19:27–37 **(in Chinese with English abstract)**

Sun SS, McDonough WF (1989) Chemical and isotopic systematics of oceanic basalts: implications for mantle composition and processes. In: Saunders AD, Norry MJ (eds) Magmatism in the Ocean Basins. Geological Society of London Special Publication, London, 42, pp 313–435. doi:10.1144/gsl.sp.1989.042.01.19

Sun WH, Zhou MF, Gao JF, Yang YH, Zhao XF, Zhao JH (2009) Detrital zircon U–Pb geochronological and Lu–Hf isotopic constraints on the Precambrian magmatic and crustal evolution of the western Yangtze Block, SW China. Precambrian Res 172(1):99–126. doi:10.1016/j.precamres.2009.03.010

Sun Y, Lai X, Wignall PB, Widdowson M, Ali JR, Jiang H, Wang W, Yan C, Bond DPG, Védrine S (2010) Dating the onset and nature of the Middle Permian Emeishan large igneous province eruptions in SW China using conodont biostratigraphy and its bearing on mantle plume uplift models. Lithos 119(1):20–33. doi:10.1016/j.lithos.2010.05.012

Tran TH, Lan C-Y, Usuki T, Shellnutt JG, Pham TD, Tran TA, Pham NC, Ngo TP, Izokh A, Borisenko A (2015) Petrogenesis of Late Permian silicic rocks of Tu Le basin and Phan Si Pan uplift (NW Vietnam) and their association with the Emeishan large igneous province. J Asian Earth Sci 109:1–19. doi:10.1016/j.jseaes.2015.05.009

Turner S, Foden J, Morrison R (1992) Derivation of some A-type magmas by fractionation of basaltic magma: an example from the Padthaway Ridge, South Australia. Lithos 28(2):151–179. doi:10.1016/0024-4937(92)90029-x

Usuki T, Lan C-Y, Tran TH, Pham TD, Wang K-L, Shellnutt GJ, Chung S-L (2015) Zircon U–Pb ages and Hf isotopic compositions of alkaline silicic magmatic rocks in the Phan Si Pan-Tu Le region, northern Vietnam: identification of a displaced western extension of the Emeishan Large Igneous Province. J Asian Earth Sci 97:102–124. doi:10.1016/j.jseaes.2014.10.016

Wang XL, Zhou JC, Griffin WA, Wang RC, Qiu JS, O'Reilly S, Xu X, Liu XM, Zhang GL (2007) Detrital zircon geochronology of Precambrian basement sequences in the Jiangnan orogen: dating the assembly of the Yangtze and Cathaysia Blocks. Precambrian Res 159(1):117–131. doi:10.1016/j.precamres.2007.06.005

Wang LJ, Yu JH, Griffin W, O'Reilly S (2012) Early crustal evolution in the western Yangtze Block: evidence from U–Pb and Lu–Hf isotopes on detrital zircons from sedimentary rocks. Precambrian Res 222:368–385. doi:10.1016/j.precamres.2011.08.001

Watson EB (1996) Dissolution, growth and survival of zircons during crustal fusion: kinetic principles, geological models and implications for isotopic inheritance. Geol Soc Am Spec Pap 315:43–56. doi:10.1130/0-8137-2315-9.43

White R, McKenzie D (1989) Magmatism at rift zones: the generation of volcanic continental margins and flood basalts. J Geophys Res Solid Earth (1978–2012) 94(B6):7685–7729. doi:10.1029/jb094ib06p07685

Wignall P, Védrine S, Bond D, Wang W, Lai XL, Ali J, Jiang HS (2009) Facies analysis and sea-level change at the Guadalupian–Lopingian Global Stratotype (Laibin, South China), and its bearing on the end-Guadalupian mass extinction. J Geol Soc 166(4):655–666. doi:10.1144/0016-76492008-118

Williams IS (1998) U–Th–Pb geochronology by ion microprobe. Rev Econ Geol 7(1):1–35

Wu P, Liu S, He B, Dou G (2015) Stratigraphic records of the dynamic uplift of the Emeishan large igneous province. Int Geol Rev. doi:10.1080/00206814.2015.1065515

Xiao L, Xu Y, Mei H, Zheng Y, He B, Pirajno F (2004) Distinct mantle sources of low-Ti and high-Ti basalts from the western Emeishan large igneous province, SW China: implications for plume–lithosphere interaction. Earth Planet Sci Lett 228(3):525–546. doi:10.1016/j.epsl.2004.10.002

Xu Y, Chung SL, Jahn B, Wu G (2001a) Petrologic and geochemical constraints on the petrogenesis of Permian–Triassic Emeishan flood basalts in southwestern China. Lithos 58(3):145–168. doi:10.1016/s0024-4937(01)00055-x

Xu YG, Luo ZY, Huang XL, He B, Xiao L, Xie LW, Shi YR (2008) Zircon U–Pb and Hf isotope constraints on crustal melting associated with the Emeishan mantle plume. Geochim Cosmochim Acta 72(13):3084–3104. doi:10.1016/j.gca.2008.04.019

Xu YG, Chung SL, Shao H, He B (2010) Silicic magmas from the Emeishan large igneous province, Southwest China: petrogenesis and their link with the end-Guadalupian biological crisis. Lithos 119(1):47–60. doi:10.1016/j.lithos.2010.04.013

Yunnan Bureau of Geology (YBG) (1966) The report of regional geological survey at scale 1:200000. Chinese Industry Press, Heqing **(in Chinese)**

Yunnan Bureau of Geology (YBG) (1973) The report of regional geological survey at scale 1:200000. Chinese Industry Press, Dali **(in Chinese)**

Yunnan Bureau of Geology (YBG) (1977) The report of regional geological survey at scale 1:200000. Chinese Industry Press, Lijiang **(in Chinese)**

Zhang Z, Mahoney JJ, Mao J, Wang F (2006) Geochemistry of picritic and associated basalt flows of the western Emeishan flood basalt province, China. J Petrol 47(10):1997–2019. doi:10.1093/petrology/egl034

Zhang Z, Mao J, Saunders AD, Ai Y, Li Y, Zhao L (2009) Petrogenetic modeling of three mafic–ultramafic layered intrusions in the Emeishan large igneous province, SW China, based on isotopic and bulk chemical constraints. Lithos 113(3):369–392. doi:10.1016/j.lithos.2009.04.023

Zheng YF, Zhang SB, Zhao ZF, Wu YB, Li X, Li Z, Wu FY (2007) Contrasting zircon Hf and O isotopes in the two episodes of Neoproterozoic granitoids in South China: implications for growth and reworking of continental crust. Lithos 96(1):127–150. doi:10.1016/j.lithos.2006.10.003

Zhong H, Zhu WG, Chu ZY, He DF, Song XY (2007) SHRIMP U–Pb zircon geochronology, geochemistry, and Nd–Sr isotopic study of contrasting granites in the Emeishan large igneous province, SW China. Chem Geol 236(1):112–133. doi:10.1016/j.chemgeo.2006.09.004

Zhong H, Zhu WG, Hu RZ, Xie LW, He DF, Liu F, Chu ZY (2009) Zircon U–Pb age and Sr–Nd–Hf isotope geochemistry of the Panzhihua A-type syenitic intrusion in the Emeishan large igneous province, southwest China and implications for growth of juvenile crust. Lithos 110(1):109–128. doi:10.1016/j.lithos.2008.12.006

Zhong H, Campbell IH, Zhu WG, Allen CM, Hu RZ, Xie LW, He DF (2011) Timing and source constraints on the relationship between mafic and felsic intrusions in the Emeishan large igneous province. Geochim Cosmochim Acta 75(5):1374–1395. doi:10.1016/j.gca.2010.12.016

Zhong YT, He B, Mundil R, Xu YG (2014) CA-TIMS zircon U–Pb dating of felsic ignimbrite from the Binchuan section: implications for the termination age of Emeishan large igneous province. Lithos 204:14–19. doi:10.1016/j.lithos.2014.03.005

Zhou MF, Yan DP, Kennedy AK, Li Y, Ding J (2002) SHRIMP U–Pb zircon geochronological and geochemical evidence for Neoproterozoic arc-magmatism along the western margin of the Yangtze Block, South China. Earth Planet Sci Lett 196(1):51–67. doi:10.1016/s0012-821x(01)00595-7

Zhou MF, Ma Y, Yan DP, Xia X, Zhao JH, Sun M (2006a) The Yanbian terrane (Southern Sichuan Province, SW China): a Neoproterozoic arc assemblage in the western margin of the Yangtze block. Precambrian Res 144(1):19–38. doi:10.1016/j.precamres.2005.11.002

Zhou MF, Yan DP, Wang CL, Qi L, Kennedy A (2006b) Subduction-related origin of the 750 Ma Xuelongbao adakitic complex (Sichuan Province, China): implications for the tectonic setting of the giant Neoproterozoic magmatic event in South China. Earth Planet Sci Lett 248(1):286–300. doi:10.1016/j.epsl.2006.05.032

Zhou MF, Arndt NT, Malpas J, Wang CY, Kennedy AK (2008) Two magma series and associated ore deposit types in the Permian Emeishan large igneous province, SW China. Lithos 103(3):352–368. doi:10.1016/j.lithos.2007.10.006

Zhu B, Guo Z, Liu R, Liu D, Du W (2014) No pre-eruptive uplift in the Emeishan large igneous province: new evidences from its 'inner zone', Dali area, Southwest China. J Volcanol Geotherm Res 269:57–67. doi:10.1016/j.jvolgeores.2013.11.015